12-2018

Computational Quantum Chemistry Studies of the Interactions of Amino Acids Side Chains with the Guanine Radical Cation.

Edward Acheampong
East Tennessee State Universtiy

Computational Quantum Chemistry Studies of the Interactions of Amino Acids Side Chains with the Guanine Radical Cation

_____

A thesis

presented to

the faculty of the Department of Chemistry

East Tennessee State University

In partial fulfillment

of the requirements for the degree

Master of Science in Chemistry

_____

by

Edward Acheampong

December 2018

_____

Dr. David Close, Chair

Dr. Scott Kirkby

Dr. Ismail Kady

Keywords: Guanine Radical Cation, Cysteine, Tyrosine, Histidine, Tryptophan, Proton/Electron Transfer, Spin Density, Density Functional Theory

ABSTRACT

Computational Quantum Chemistry Studies of the Interactions of Amino Acids Side Chains with the Guanine Radical Cation,

by

Edward Acheampong

Guanine is generally accepted as the most easily oxidized DNA base when cells are subjected to ionizing radiation, photoionization or photosensitization. At pH 7, the midpoint reduction potential is on the order of 0.2 – 0.3 V higher than those of the radicals of e.g. tyrosine, tryptophan cysteine and histidine, so that the radical "repair" (or at least, a thermodynamically favorable reaction) involving these amino acids is feasible. Computational quantum studies have been done on tyrosine, tryptophan, cysteine and histidine side chains as they appear in histones. Density functional theory was employed using B3LYP/6-31G+ (d, p) basis set to study spin densities on these amino acids side chains as they pair with the guanine radical cation. The amino acid side chains are positioned so as not to disrupt the Watson-Crick base pairing. Our results indicate that, these side chains of amino acid with reducing properties can repair guanine radical cation through electron transfer coupled with proton transfer.

DEDICATION

To my father Mr. Thomas Acheampong, my mother Mrs. Rose Acheampong, and my entire family

ACKNOWLEDGMENTS

I am grateful to the almighty God for His guidance and protection over me and the blessing He has bestowed upon me. I would also like to thank my advisor Dr. David M. Close for his patience, understanding, his professional guidance and mentorship. My profound gratitude goes to Dr. Scott Kirkby and Dr. Ismail Kady for serving on my committee and for their advice. I will also like to express my appreciation to Extreme Science and Engineering Discovery Environment (XSEDE) Organization for the computer time allocation given to me and my advisor for us to be able to complete this work. I also owe my gratitude to Mahidhar Tatineni and Jerry Greenberg, all at San Diego Super Computer Center for helping me on comet. I thank all the staff of the Chemistry Department of ETSU. My sincere gratitude goes to Mrs. Ida Aseidu, Accra, Ghana, for all her financial support. I thank all graduate students in the Chemistry Department, especially Mr. George Affadu Danful and Mr. Theophilus Neequaye, for all their help.

TABLE OF CONTENTS

LIST OF TABLES

Table Page

LIST OF FIGURES

Figure Page

CHAPTER 1

INTRODUCTION

Oxidative Stress and DNA

Aerobic organisms make use of oxygen for the oxidation of biological molecules for their survival, to promote cellular signaling and other important process.[1] However, research has proven that excessive oxidation of these molecules can cause an oxidative stress which can harm the organism.[2] The genome, which stores all genetic information is constantly assaulted by endogenous and exogenous oxidative stress. The various exogenous insults that contribute to the overproduction of oxidizing species in the cells that can cause oxidative stress include environmental pollution,[3] UV light,[4] ionizing radiation,[5] and tobacco smoke.[6] Reactive oxygen species (ROS) are species capable of inducing oxidation and they include hydrogen peroxide (H_2O_2), the superoxide radical ($O_2^{\bullet-}$), nitric oxide (NO), hydroxyl radical ($HO^{\bullet}$), peroxynitrite ($ONOO^-$), and several others which are usually free radicals. Overproduction of ROS has been shown to link to many diseases such as cancers,[7] inflammatory diseases,[8] ischemia and reperfusion,[9] some neurodegenerative diseases like Huntington's disease,[3] and Alzheimer's disease.[10] Of all the biomolecules which are subjected to oxidative stress, deoxyribonucleic acid (DNA) damage which is also caused by oxidative stress has been investigated frequently since it is the major hereditary molecule for all species.[8,9] The interaction of DNA with ROS can lead to several oxidative modifications in the DNA including damage to the deoxyribose moiety of the sugar-phosphate backbone of the DNA double helix, intrastrand crosslinks, nucleobase modifications, single-strand and double-strand breaks (SSBs and DSBs), and DNA-protein crosslinks.[11] These modifications in DNA are usually easily repaired by

cellular processes. During oxidative stress, the number of lesions is too large for cellular DNA repair. These mechanisms are unable to repair some of these modifications which are then left unrepaired. In fact, these unrepaired or improperly repaired modifications are the cause of many of the diseases and conditions mentioned earlier. This is because unrepaired or improperly repaired DNA modifications accumulate, which gradually leads to the development of these maladies.

Ionizing Radiation

Ionizing radiation is radiation with photon energy of more than 1215 kJ/mol, which by definition is equal to the ionization energy of a water molecule. When ionizing radiation interacts with matter, two major events usually occur: ionization and electronic excitation. When a molecule M is ionized, an electron is removed and thus, a positively charged radical cation is formed:

$$M + h\nu \rightarrow M^{\bullet +} + e^{-} \quad (1.1)$$

In the case of electronic excitation, the ionizing radiation promotes an electron from a lower occupied orbital in molecule M to an empty unoccupied orbital of higher energy to form an excited molecule M*.

$$M + h\nu \rightarrow M^{*} \quad (1.2)$$

Even though there are other sources of oxidative stress, as reported earlier, ionizing radiation has been one of the most important sources of oxidative stress in biological systems. Ionizing radiation has always been part of the human environment. In addition to natural radiation sources present in the earth's crust, cosmic and solar radiation; man-made sources have also been a contributing factor to our unceasing exposure to radiation. The ionization of biomolecules in which water molecules play a

vital role can produce oxidative species including ROS which can induce oxidative damage in living cells.[12]

Two types of radiation damage to DNA have been identified: direct and indirect.[13] Direct damage involves the ionization of DNA by ionizing radiation while indirect involves the interaction of DNA with radicals produced by ionizing radiation of water molecules or other molecules in the surrounding medium.[13]

Oxidative Damage to DNA by Indirect Effects

Oxidative damage to DNA by indirect effects occurs when a reactive oxygen species attacks the DNA. This can either be on a nucleobase or the deoxyribose-phosphate backbone. Damage to the deoxyribose-phosphate moiety is usually related to SSBs and DSBs, and these types of damage have been generally accepted as important biomarkers for cellular DNA damage.[11] SSBs and DSBs are also considered to be mutagenic in nature because of the possibility of base deletion which can easily occur during natural repair process, for instance, non-homologous recombination.[14] Due to the lower reduction potential of the nucleobase moiety than the deoxyribose moiety, nucleobases are more prone to oxidative damage. These oxidative nucleobase lesions can occur through the direct and/or indirect effect of ionizing radiation. Guanine in most cases is highly affected due to its lowest reduction potential. Positively charged electron-loss centers (holes) in the DNA structure due to oxidizing agents will automatically end up at guanine base because of charge transfer in DNA.[15] Table 1 shows the reduction potentials of some nitrogenous bases.

Table 1: Relative standard potentials for nitrogenous bases[16]

DNA Nucleosides	E°, V
Guanine	1.29
Adenosine	1.42
Thymidine	1.7
Cytidine	1.6

Oxidative Damage to the Guanine Base

Guanine undergoes two major oxidation pathways, as a result of which a large number of intermediates are formed,[17] mechanisms of formation of these intermediates and final products are not fully understood.[17] In the first pathway, there is a double-bond attachment when the free radical adducts are formed, as in the reaction with hydroxyl radical, and in the second there is a reaction with an one-electron oxidant (OEO). The hydroxyl radical is a very reactive species, the mechanism of its reaction with a guanine base has been studied more intensely than other oxidation reaction of guanine.[18]

The first pathway of guanine oxidation involves the attack of the hydroxyl radical ($OH^{\bullet}$) on one of the two guanine carbons, C4 or C8, to form $G(OH^{\bullet})$ as shown in **12** of Figure 1**.** The hydroxyl radical will preferentially attack the C8 carbon of the purine ring forming the intermediate $G(OH^{\bullet})$ which can either be oxidized to form 8-oxoguanine (8-oxoG)[19] or reduced to form 2,6-diamino-4-hydroxy-5-formamidopyrimidine (FapyG) **14.**[20] If the hydroxyl radical attacks the C4 carbon followed by a dehydration reaction, a neutral radical ($G^{\bullet}$) is formed. According to Cadet *et al*., $G^{\bullet}$ can react with molecular oxygen to form 2-amino-5-[(2-deoxy-β-D-erythro-pentofuranosyl) amino]-4H-imidazol-

4-one (imidazolone or Iz) **17**.[21] As Iz is unstable, it will hydrolyze to form 2,2-diamino-4-[(2-deoxy-β-D-erythro-pentofuranoxyl) amino]-2,5-dihydrooxazol-5-one (oxazolone or Oz) **18**.[21] Figure 1 shows the summary of these oxidation processes.

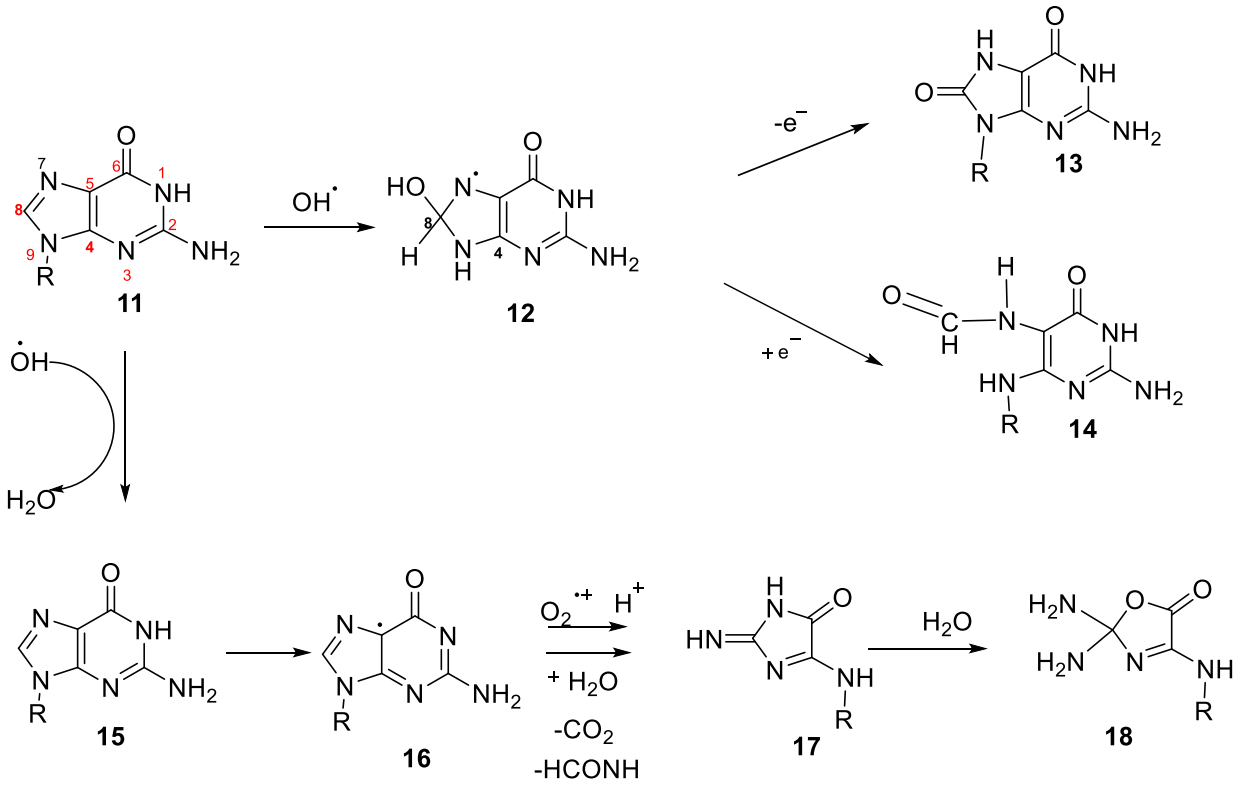

Figure 1: Hydroxyl radical-mediated oxidation of the guanine moiety in DNA. This is adapted from a similar scheme found in Cadet *et al.*[21]

The second pathway involves reactions of guanine with various one-electron oxidants such as the carbonate radical anion ($CO_3^{\bullet-}$), the sulfate radical anion ($SO_4^{\bullet-}$), dibromide radical anion (Br^-), or photoexcited riboflavin. While $SO_4^{\bullet-}$ is a strong oxidant ($E° = 2.43$ V) and will rapidly oxidized any free nucleoside, the carbonate and dibromide radical anions are weaker oxidants ($E° = 1.59$ V and 1.62 V, respectively) and will only oxidize guanine.[22] Oxidation base lesions occurs primarily on guanine, which leads to a

one-electron oxidation intermediate guanine radical cation ($G^{\bullet+}$). The $G^{\bullet+}$ is a stronger acid than G itself with a pKa of 3.9 and at a physiological pH, it quickly undergoes deprotonation to form $G^{\bullet}$. The $G^{\bullet}$ radical is very unstable and it has not been detected at room temperature[23] as it decays rapidly in the 120-230 K temperature range.[23] It has therefore been hypothesized that $G^{\bullet}$ undergoes a second one-electron oxidation to form the carbocation $G(N1\text{-}H)^{+}$.[23]Another proposed idea is that, $G^{\bullet+}$ can react with water to form $G(OH)^{\bullet}$ radical and that this radical can proceed down one of two pathways: a second one-electron oxidation to form 8-oxoG.[23] Figure 2 shows these reactions.

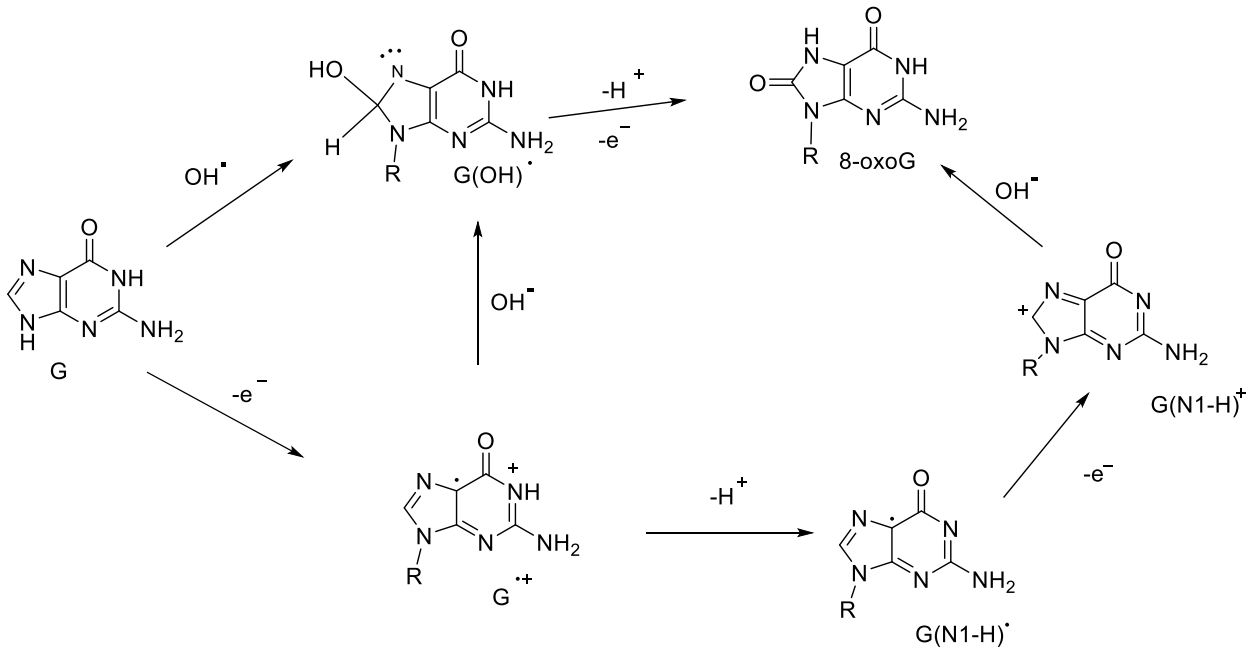

Figure 2: Reactions and products of guanine oxidation. This scheme is adapted from a scheme found in Close *et al.*

Direct Type DNA Damage

Direct damage of DNA by ionizing radiation has been studied in dry samples of DNA[24] using X-ray crystallography,[25] neutron scattering,[26] nuclear magnetic resonance

(NMR) spectroscopy,[27] electronic[28] and vibrational spectroscopy,[29] molecular dynamics[30] and electron paramagnetic resonance spectroscopy (EPR).[31] Dry DNA still contains some water molecules in its solvation shell. NMR experiments have measured different time scales concerning the dynamics of water in the solvation structure of DNA,[32] and time resolved fluorescence measurements have suggested evidence of water molecules in the hydration shell,[33] but the interpretation of the latter measurements has been questioned.[34] The solvation shell of DNA consists of about 22 water molecules per nucleotide. Approximately 2.5 water molecules per DNA nucleotide are tightly bound to DNA and are not removable even under harsh conditions.[35] DNA hydration Γ is evaluated as the number of water molecules per DNA nucleotide. Basically, one cannot detect $OH^{\bullet}$ radicals at low DNA hydration ($\Gamma < 8$).[36] This means that in the first step of ionization, the hole produced in the DNA solvation shell transfers to DNA. It is not possible to distinguish the products of DNA damage resulting from hole transfer from the solvation shell and those resulting from the direct ionization of DNA. For that reason, the direct type of damage is usually considered to rise from direct ionization of DNA or from the transfer of holes from the DNA solvation shell. It is therefore necessary to view DNA and its solvation shell as a single target. Therefore, the general ideal of direct ionization of DNA can be describe by the equation below.

$$DNA + h\nu \rightarrow DNA^{\bullet+} + e^{-} \text{ (oxidation)} \quad (1.3)$$

$$DNA + e^{-} \rightarrow DNA^{\bullet-} \text{ (reduction)} \quad (1.4)$$

Proton and Electron Transfer in DNA

In the past decade, long-distance charge transfer mediated by DNA has received considerable experimental[37] and theoretical attention.[38] Theoretical methods provide a

variety of quantitative measurements that are difficult to obtain experimentally and allow one to consider in detail different factors that control the charge transfer process. Although the main aspect of electron transfer (ET) in DNA is now well understood *in vitro*, many important mechanistic details on ET in genomic DNA remain to be explored. It has been experimentally found that protein-nucleic acid interactions in nucleosome core particles (NCP) can considerably influence the ET process[39] and therefore theoretical studies of related models are of special interest. Using a relatively simple quantum mechanical approach, Koslowski and coworkers studied the migration of a radical cation through DNA in NCP.[40] They suggested that damage to DNA in NCP may occur because of charge transfer from an unprotected DNA segment to the histone-coordinated sequence. Therefore, to protect the genome some mechanisms should exist that prevent the effective hole transfer within the DNA stack. The repair of this species implies both electron and proton transfer reactions. This mechanism has been recently studied in detail by Density Functional Theory (DFT).[41]

Some Amino Acids with Reducing Properties

In protein-DNA complexes, an amino acid residue Y that has a lower oxidation potential than guanine G, can act as electron donor (or, equivalently acceptor hole) retrieving the native state of the guanine from its radical cation.[42]

$$G^{\bullet+} + Y \rightarrow G + Y^{\bullet+} \qquad (1.5)$$

This ET reaction should prevent possible damage to DNA. The low oxidation potentials of these amino acids make the repair of G feasible, as has been observed for different systems in aqueous solutions,[43] DNA-tripeptide, and DNA-protein complexes.[44] In particular, charge migration in DNA is shown to decrease remarkably with its binding

by endonuclease.[45] Significant difference in the dynamics of DNA-mediated hole transport in the presence and absence of packaging into NCP has been reported.[46] In NCP there are numerous close contacts between DNA and amino acid residues,[47] which should make possible the electron transfer reaction from the amino acid to the guanine. It is observed that electrostatic interactions between nucleobase and surrounding amino acid residues affect the stability of guanine. Thus, the standard oxidation potential of the amino acid and the guanine provides only rough estimates for the ET free energy. The hole trapping process can be accompanied by proton transfer. The formation of radical cation Y leads to a decrease of its pKa-value and can enforce rapid deprotonation of the residue due to proton transfer to the surroundings. As a result, back ET from G to Y becomes unfeasible. The six most easily oxidized amino acids (the six best reducing agents) are cysteine, cystine, histidine, methionine, tryptophan, and tyrosine.[48] The reduction potentials of these amino acids, dipeptides containing them, and structurally very similar compounds are available in the literature. Values at pH 7 are as shown in Table 2 below.

Table 2: Standard reduction potentials of some amino acid residues at pH 7.[48]

Amino Acid Side Chains	$E_{7,}$ Volts
Cysteine	0.9
Cystine	1.1
Histidine	1.2
Tryptophan	1.0
Tyrosine	0.9
Glutathione	0.92

Again, only four of these amino acids were studied in this work and the structure of these four amino acids are listed in Figure 3 below

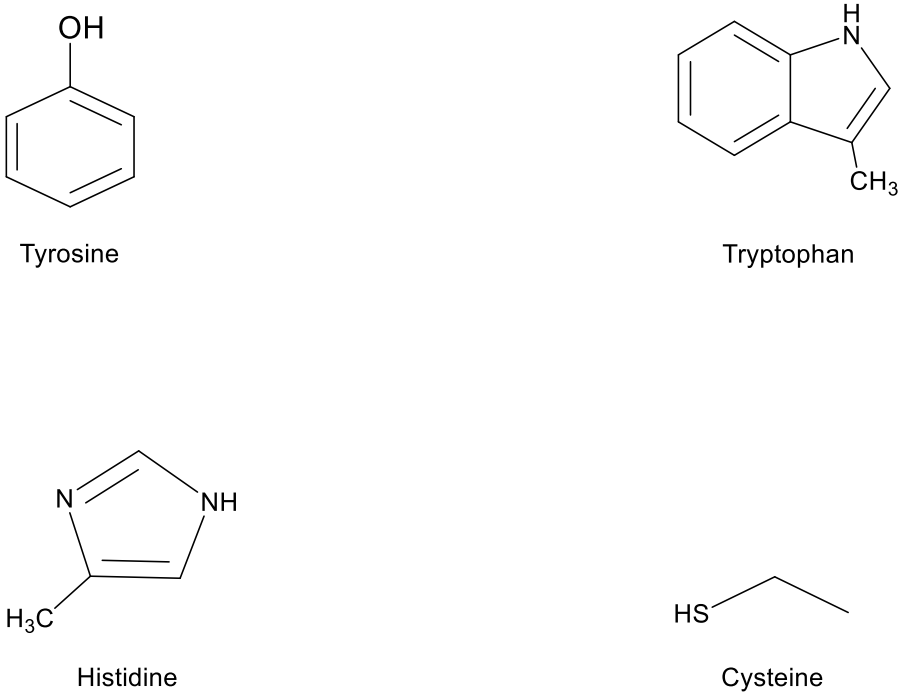

Figure 3: Chemical structures of tyrosine, tryptophan, histidine and cysteine side chains

DFT calculations have also been employed to study the stabilization process of guanine radical cation through amino acids interactions as well as to understand the protection mechanism by Jing Zhao *et al*.[49] On the basis of their calculations, several protection mechanisms were proposed to cysteine, histidine, tyrosine and tryptophan side chains. Their results indicated that amino acids with reducing properties can repair the guanine radical cation through proton-coupled electron transfer or electron transfer. Their model is with the N1-H on the guanine radical cation. Their results for cysteinyl are shown in Figure 4 below

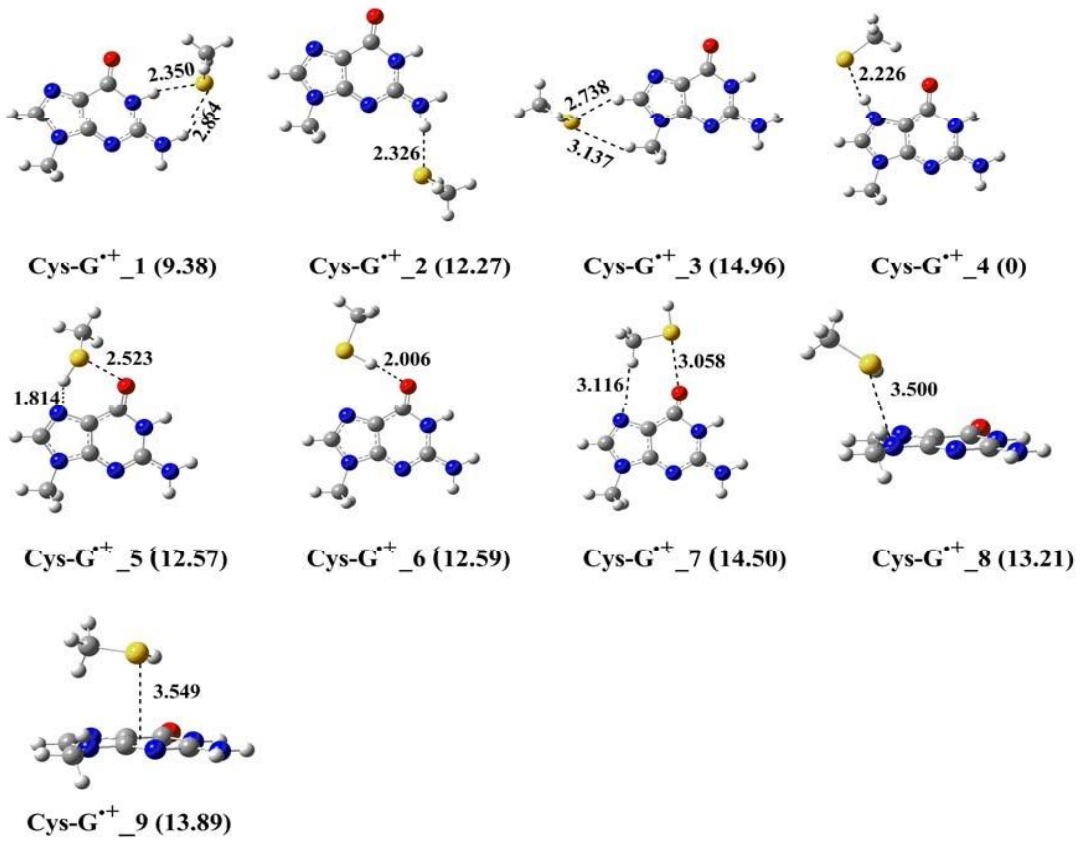

Figure 4: Geometries of the Cys- $G^{\bullet+}$ complexes obtained at the B3LYP/6-31+G** level in the gas phase.[49] The bond lengths are given in Å. The values in parentheses are the relative energies (kcal/mol) with respect to Cys- $G^{\bullet+}$_4.

The plots of the spin densities for the Cys-G$^{\bullet+}$ complexes are shown in Figure 5 below

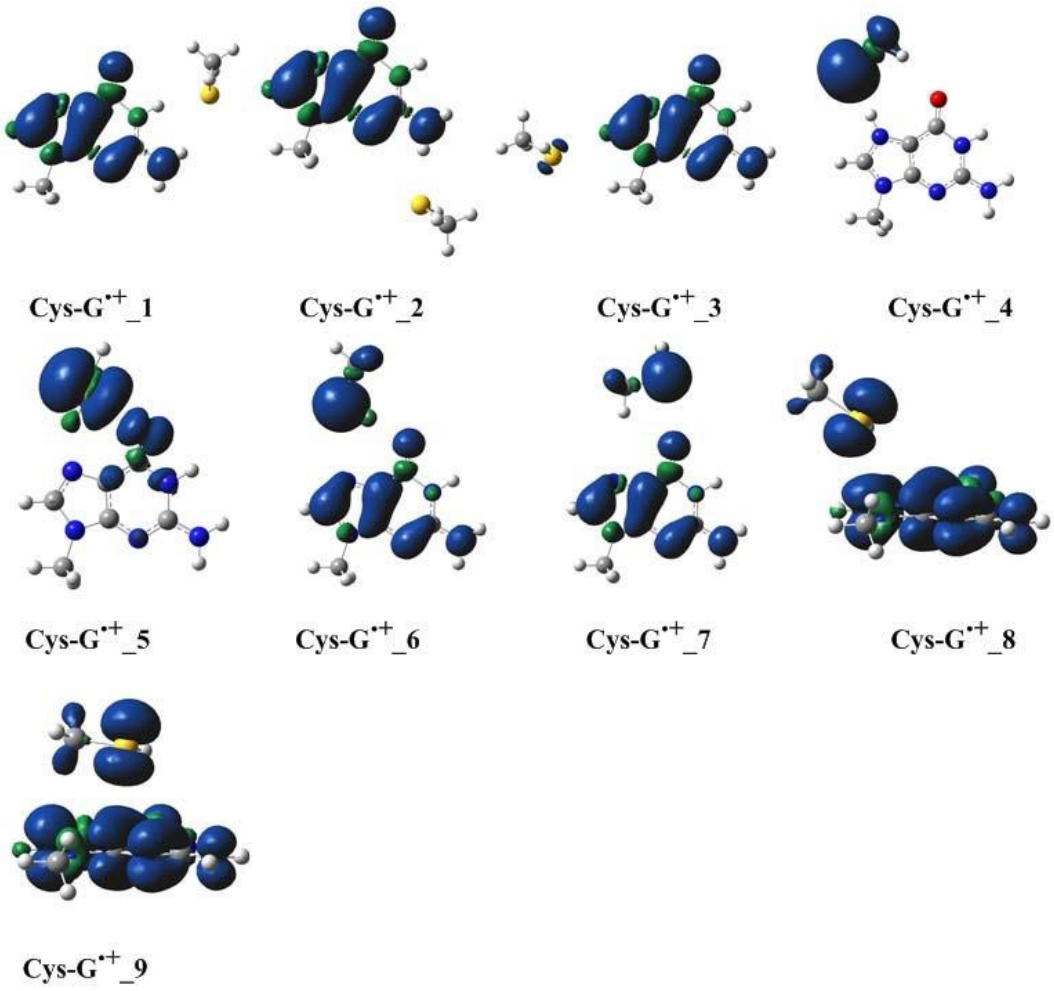

Figure 5: Plots of the spin density for the Cys- G$^{\bullet+}$ complexes[49]

Their results showed that a proton-driven partial-electron transfers occurs. For Cys-G$^{\bullet+}$, the Cys(-H)$^{\bullet}$G(H7)$^{+}$ state was more stable and the same was true for Tyr(-H)$^{\bullet}$G(H7)$^{+}$ as shown in the Figure 6 below

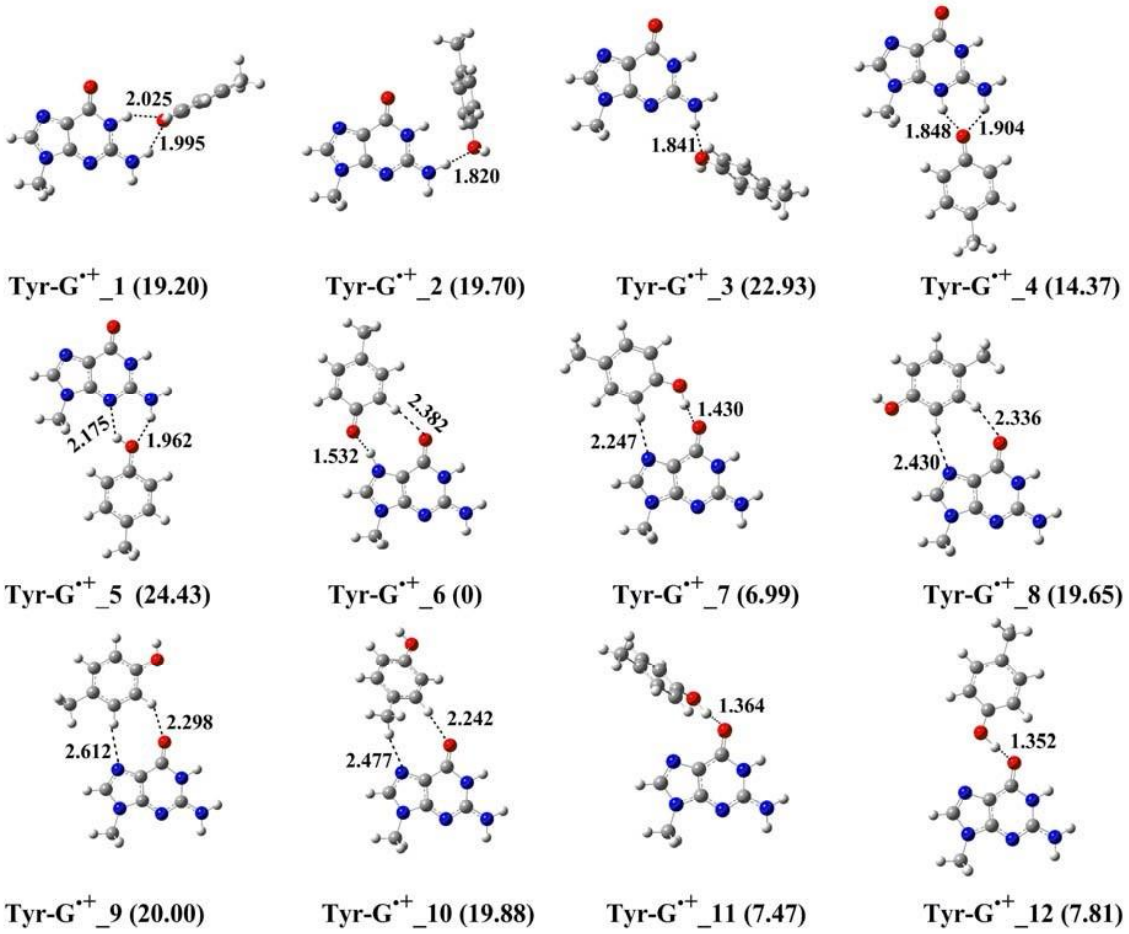

Figure 6: Geometries of the Tyr- $G^{\bullet+}$ complexes obtained at the B3LYP/6-31+G** level in the gas phase.[49] The bond lengths are in Å. The values in parentheses are the relative energies (kcal/mol) with respect to Tyr- $G^{\bullet+}$_6.

The plots of the spin density for the Tyr-$G^{\bullet+}$ complexes are also shown in Figure 7 below

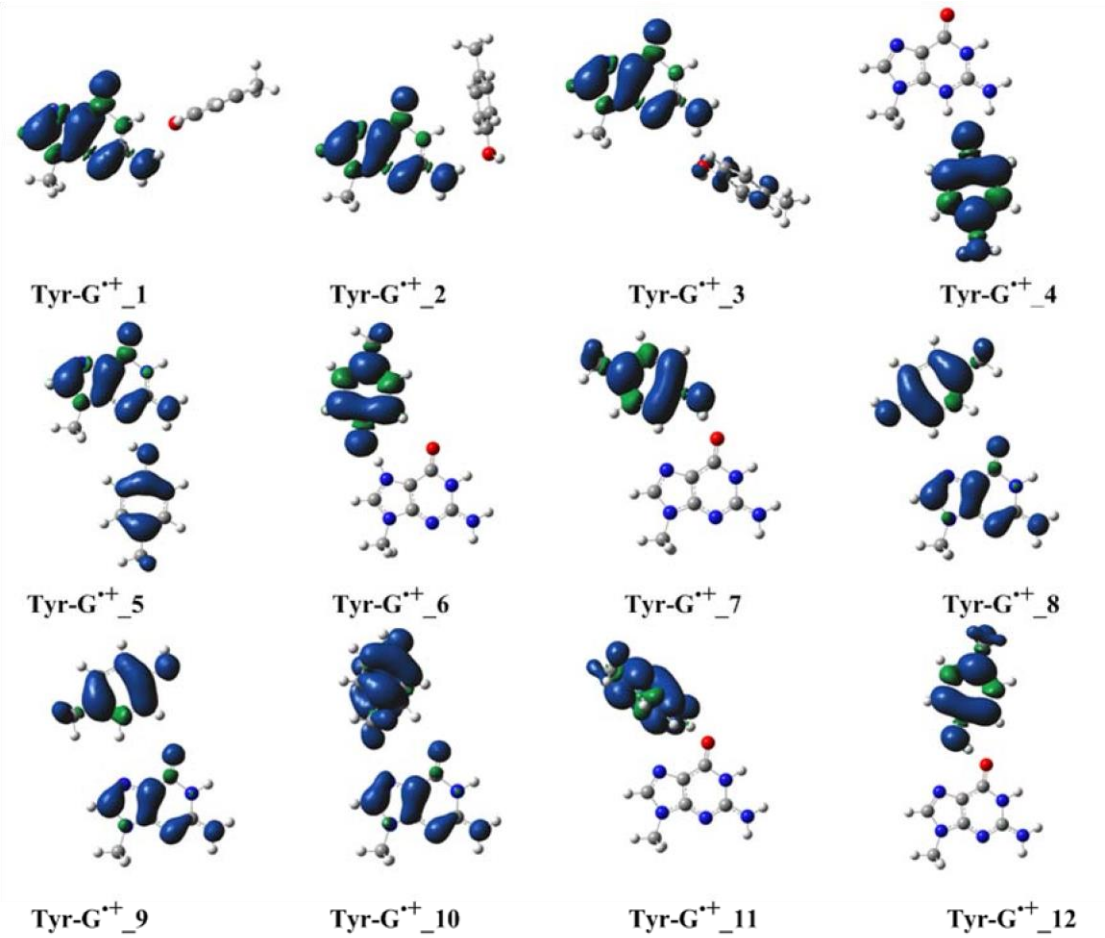

Figure 7: Plots of the spin density for the Tyr- $G^{\bullet+}$complexes.[49]

The same observations were made for histidine and tryptophan as shown in Figures 8-11 below

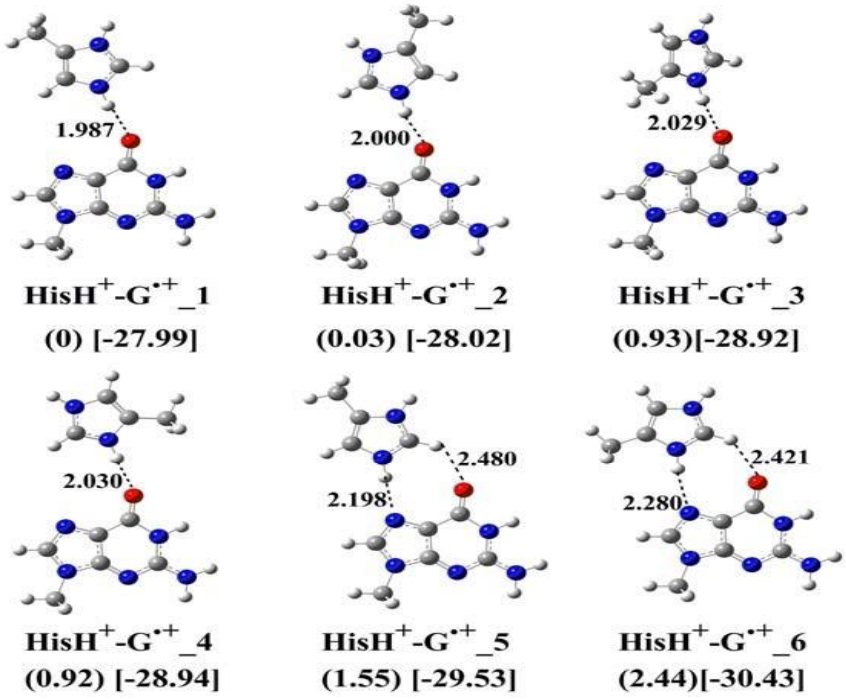

Figure 8: Geometries of the $HisH^+$- $G^{\bullet+}$ complexes obtained at the B3LYP/6-31+G** level in the gas phase.[49] The bond lengths are in Å. The values in parentheses are the relative energies (kcal/mol) with respect to $HisH^+$- $G^{\bullet+}$_1; and the numbers in brackets are dissociation energies (kcal/mol).

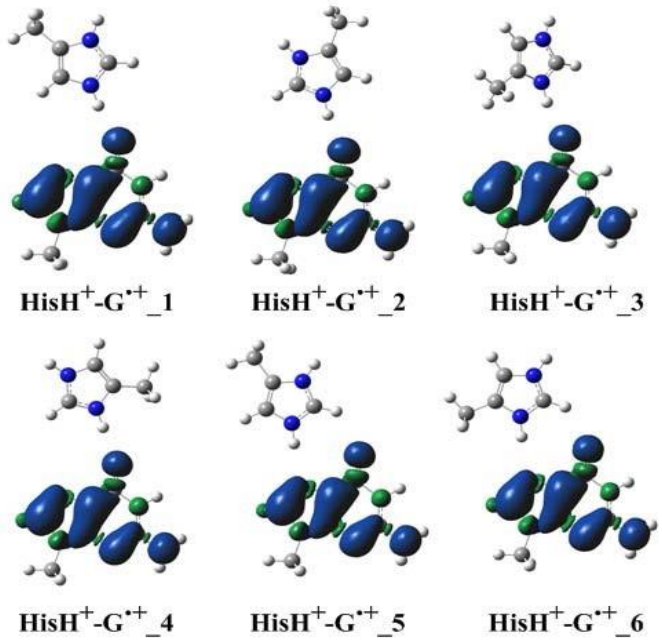

Figure 9: Plots of the spin density for the $HisH^+$- $G^{\bullet+}$ complexes.[49]

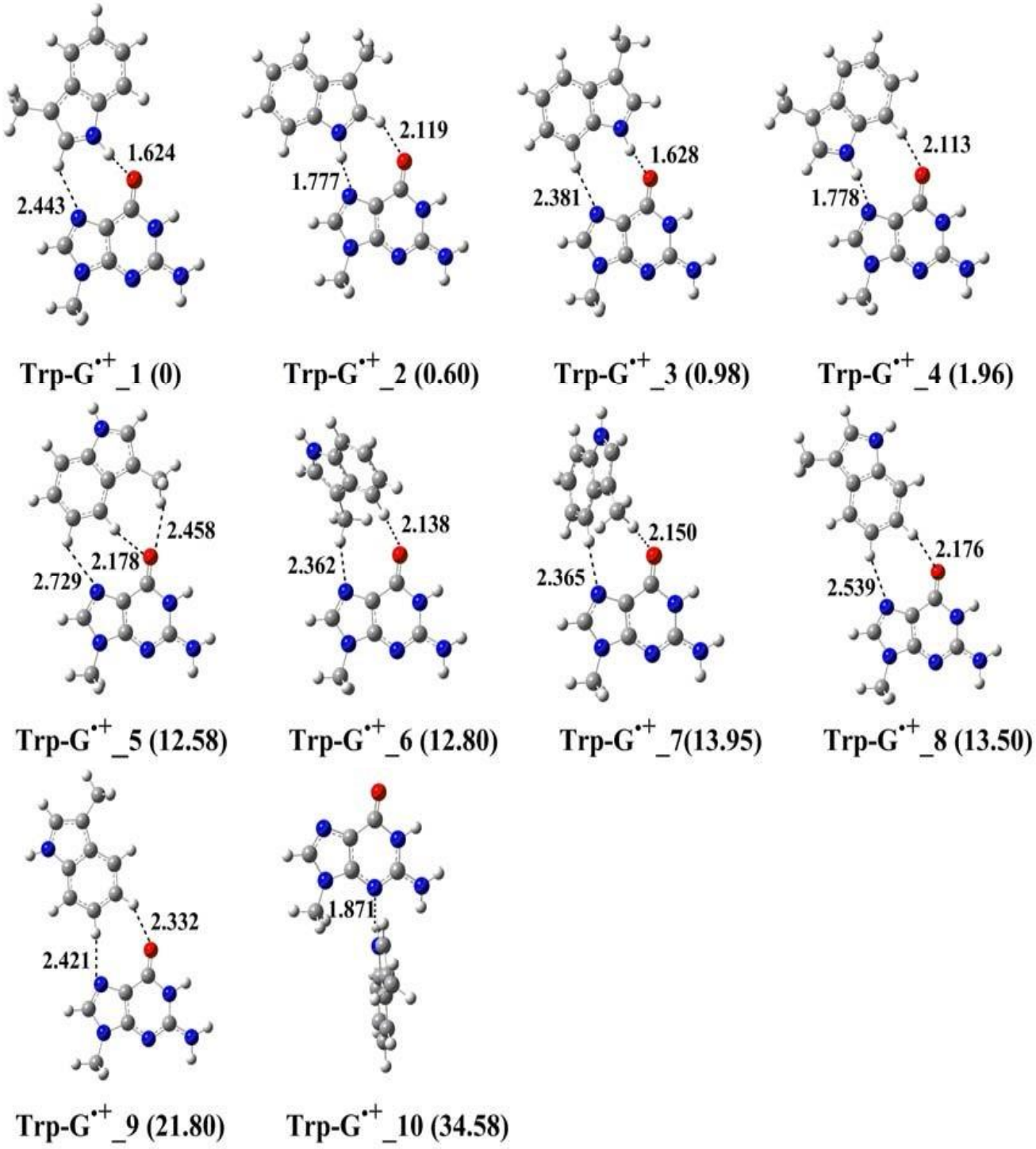

Figure 10: Geometries of the Trp- $G^{\bullet+}$complexes obtained at the B3LYP/6-31+G** level in the gas phase.[49] The bond lengths are in Å. The values in parentheses are the relative energies (kcal/mol) with respect to Trp- $G^{\bullet+}$_1.

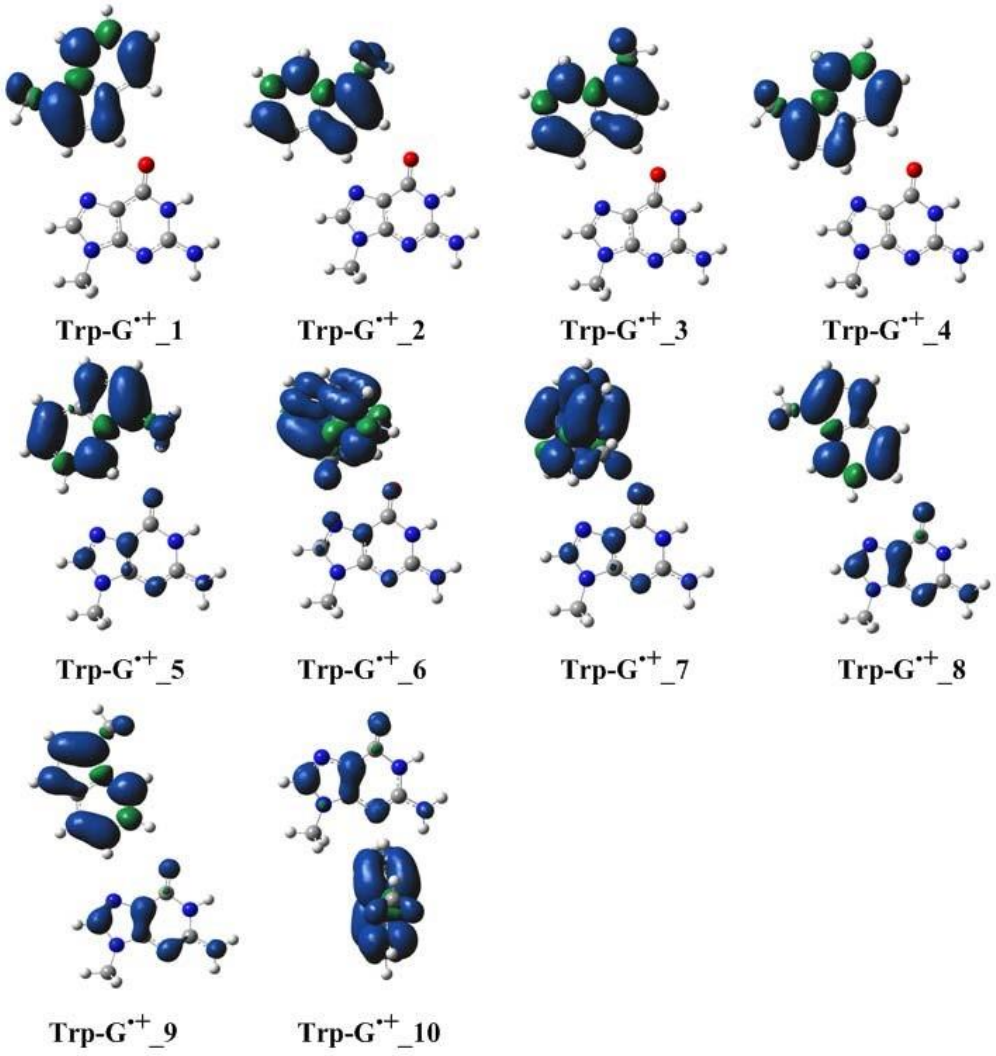

Figure 11: Plots of the spin density for the Trp-G$^{\bullet+}$ complexes.[49]

Among the considered amino acid-guanine interactions, Jing Zhao and co-researchers observed that a normal guanine can be retrieved by some interaction modes with amino acids residues.[49] That is, certain amino acids residues can help to prevent DNA damage, in particular, tryptophan, tyrosine and histidine which are aromatic amino acids that have lower ionization potentials (7.51, 8.34, 8.81 eV),[50] and may be capable of repairing the G$^{\bullet+}$ radical cation, owing to their side chains containing functional groups (indole, phenol and imidazole) with strong reducing properties.

However, it was observed in their work that most of their geometries had the tendency of disrupting the Watson-Crick base pairing. This work was based on the fact that at physiological pH, the pKa of the guanine radical cation is 3.9 which can only be obtained when the N1-H of the guanine radical cation is ignored. Again, the geometries of this work are representative of some of the geometries of Jing Zhao and coworkers e g. Cys-$G^{\bullet+}$_6, Tyr-$G^{\bullet+}$_7 $HisH^{+}$-$G^{\bullet+}$_2 and Trp-$G^{\bullet+}$_1 were like the geometries that were optimized for cysteine, tyrosine, histidine and tryptophan side chain with guanine radical cation respectively.

.

CHAPTER 2

QUANTUM MECHANICS

Introduction to Quantum Mechanics

Quantum mechanics is the theoretical framework within which it has been found possible to describe, correlate and predict the behavior of a vast range of physical systems. The description of motions of macroscopic objects that was discovered in the late seventeenth century by classical mechanics could not correctly describe the motion of microscopic objects. This is as a result of continuous energy variations in classical mechanics; however, the behavior of small particles such as electrons, was first observed through blackbody radiation curves and the photoelectric effects.[51] This behavior can only be correctly described by a set of laws called quantum mechanics. This led to the development of quantum mechanics. Quantum mechanics utilizes a state function (or wave function) Ψ that contains all possible information about a system.[51] The wave function describes the state of a particle and is a function of both a particle's position and time, $\Psi(x, t)$. Since microscopic particles behave as particles and waves, it imposes a limit on the ability to measure simultaneously the position and momentum of such particles.[51] The more precise we determine the position the less accurate is our determination of momentum and the vice versa. This limitation is called the uncertainty principle, discovered by Werner Heisenberg in 1927.[51] Because of wave-particle duality, the act of measurement introduces an uncontrollable disturbance in the system being measured which changes the state of the system. Therefore, while future states and motions can be calculated from knowing the state of a system at any time in classical

mechanics, the exact future states and motions of particles cannot be determined in quantum mechanics.

Time-Dependent Schrödinger Equation

The concept of the wave function and the time-dependent equation was developed by Erwin Schrödinger. His approach to quantum mechanics was to postulate the basic principles and then use these postulates to deduce experimentally testable consequences, and so he postulated Ψ and by making use of Newtons second law[52] he came out with the time dependent equation that describes how the wave function changes over time.[52] The time-dependent Schrödinger equation is:

$$-\frac{\hbar^2}{2m}\frac{\partial^2\Psi(x,t)}{\partial x^2} + V(x,t)\Psi(x,t) = \frac{\hbar}{i}\frac{\partial\Psi(x,t)}{\partial t} \qquad (2.1)$$

where i is the imaginary operator $(\sqrt{-1})$, $\hbar$ is defined as h divided by 2π, h is Planck's constant, m is the mass of the particle, and V is the potential energy operator, Ψ (x, t) is the wave function of position x and time t. The potential energy operator in the time-dependent Schrödinger equation serves to set conditions on the spatial part of the wave function. The time dependent Schrödinger equation may be used to derive the time independent Schrödinger equation.

Time-Independent Schrödinger Equation

Many applications of quantum mechanics to chemistry do not use the time-dependent Schrödinger equation even though looks formidable.[51] However, the simpler time-independent Schrödinger equation describes many applications of quantum

mechanics in chemistry. It is therefore important to separate the time dependent Schrödinger equation into the time independent Schrödinger equation for one dimension and the relationship for time evolution of the wave function. If we restrict our self to a special case where no time-dependent external forces are exerted on the system, then the potential energy is not a function of time but depends only on the particle's position,$V(x)$. The wave function can be written as the product of a function of time $f(t)$ and a function of $\Psi(x)$.

$$\Psi(x,t) = f(t)\psi(x) \tag{2.2}$$

Ψ is used for the time-dependent wave function and ψ used for the factor that depends only on the coordinate *x.* Equation 2.2 can be partially differentiated and substitution into Equation 2.1 yields Equation 2.3

$$-\frac{\hbar}{i}\frac{df(t)}{dt}\psi(x) = -\frac{\hbar^2}{2m}f(t)\frac{d^2\psi(x)}{dx^2} + V(x)f(t)\psi(x) \tag{2.3}$$

$$-\frac{\hbar}{i}\frac{1}{f(t)}\frac{df(t)}{dt} = -\frac{\hbar^2}{2m}\frac{1}{\psi(x)}\frac{d^2\psi(x)}{dx^2} + V(x) \tag{2.4}$$

Division of Equation 2.3 by $f(t)\psi(x)$ forms Equation 2.4. The left side of Equation 2.4 is independent *x* and the right side is independent of *t*. The function must be a constant. We call this constant E, the energy of the system. Equating the right side of Equation 2.4 to E and multiplying both sides by $\psi(x)$ gives the time-independent Schrödinger equation for a particle in one dimension for a single particle of mass *m* moving in one dimension.

$$-\frac{\hbar^2}{2m}\frac{d^2\psi(x)}{dx^2} + V(x)\psi(x) = E\psi(x) \tag{2.5}$$

The Hamiltonian Operator

Levine defines an operator as "a rule that transforms a given function into another function."[51] The differentiation operator d/dx is an example. It transforms a differentiable function f(x) into another function f (x). Other examples include integration, the square root, and so forth. Numbers can also be considered as operators (they multiply a function). In quantum mechanics, physical observables (e.g., energy, momentum, position, etc.) are represented mathematically by operators. An example is the Hamiltonian operator which corresponds to energy. Sir William Rowan Hamilton developed an alternative form of Newton's equations of motion involving a function *H*, the Hamiltonian function for the system.[53] Under most circumstances this operator is assumed to be self-adjoint, thus having a real spectrum. The spectral values in such a case are interpreted as possible resulting values of an energy measurement performed on the system. The Hamiltonian operator can then be seen as synonymous with the energy operator, which serves as a model for the energy observable of the quantum system. In these two aspects of (a) generating the dynamics and (b) representing the energy observable, the Hamiltonian operator in quantum theory plays a role very much analogous to that of the Hamiltonian function in classical theories.[54] Historically this fact became obvious as soon as modern quantum mechanics was constituted by Heisenberg, Schrodinger, Dirac and others.[52] The classical-mechanical Hamiltonian function H for a single particle in one dimension turns out to be simply the total energy expressed in terms of coordinates (x, y, z) and conjugate momenta (p_x, p_y, p_z). The Hamiltonian function is equal to the energy, which is composed of kinetic and potential energy in one dimension as:

$$H = \frac{p_x^2}{2m} + V(x) \tag{2.6}$$

The first term on the right-hand side is the kinetic energy and the second term is the potential energy. The Hamiltonian operator can also be given in term of kinetic and potential energy operators, $\hat{T}$ and $\hat{V}$, respectively as.

$$\hat{H} = \hat{T} + \hat{V} = -\frac{\hbar^2}{2m}\frac{d^2}{dx^2} + V(x) \tag{2.7}$$

The only values that can be found for the energy of a system are the eigenvalues of the energy (Hamiltonian) operator $\hat{H}$. Using ψ_i to symbolize the eigenfunction of $\hat{H}$, we have the eigenvalue equation given below.

$$\hat{H}\psi_i = E_i\psi_i \tag{2.8}$$

The Schrödinger equation can be extended to three-dimensional, many particle systems. The kinetic energy operator consists of the sum of the individual kinetic energy operator's particles

$$\hat{T} = -\sum_i \frac{\hbar^2}{2m_i}\nabla_i^2 \tag{2.9}$$

Where the Laplacian operator ∇^2 is given by the equation below.

$$\nabla^2 = \frac{\partial^2}{\partial x^2} + \frac{\partial^2}{\partial y^2} + \frac{\partial^2}{\partial z^2} \tag{2.10}$$

Approximation Methods

Born-Oppenheimer Approximation

The Born-Oppenheimer approximation is an efficient approximation resulting in energies close to the actual energy of the system. The masses of the nuclei are much greater than the electrons, hence the electrons can respond almost instantaneously to any change in the nuclear positions. Thus, to a good approximation, we can consider the electrons as moving in a field of fixed nuclei. This helps us to separate the Schrödinger equation into two parts, one for the nuclei and the other for electrons. Moreover, within this approximation, the nuclear kinetic energy term can be neglected and the nuclear–nuclear repulsion term can be taken as a constant. We retain the inter-nuclear repulsion terms, which can be calculated from the nuclear charges and the inter- nuclear distances. In this approximation, we retain all terms involving electrons, including the potential energy terms due to attractive forces between the nuclei and electrons and those due to repulsive forces among electrons.

In studying molecular quantum mechanics, if we assume the nuclei (α and β) and electrons (i and j) are point masses and neglect spin-orbit and other relativistic interactions, then the molecular Hamiltonian is given as

$$\widehat{H} = -\frac{\hbar^2}{2}\sum_\alpha \frac{1}{m_\alpha}\nabla_\alpha^2 - \frac{\hbar^2}{2m_e}\sum_i \nabla_i^2 + \frac{e^2}{4\pi\varepsilon_0}\left(\sum_\alpha \sum_{\beta>\alpha} \frac{Z_\alpha Z_\beta}{r_{\alpha\beta}} + \sum_i \sum_{j>i} \frac{1}{r_{ij}} - \sum_\alpha \sum_i \frac{Z_\alpha}{r_{i\alpha}}\right) \quad (2.11)$$

where Z_α, Z_β are the atomic numbers, r is the distance between two particles, and e is the charge on a proton. The first two terms represent the sums of the kinetic energies of the nuclei and

electrons, respectively. The third term is the sum of the potential energies due to the electrostatic repulsion between two nuclei, and the fourth term is the sum of the potential energies due to the electrostatic repulsion between two electrons. The fifth term represents the sum of the potential energies due to the electrostatic attraction between an electron and a nucleus. For the H_2 molecule, the Hamiltonian operator is given by:

$$\widehat{H} = -\frac{\hbar^2}{2m_p}\left(\nabla_\alpha^2 + \nabla_\beta^2\right) - \frac{\hbar^2}{2m_e}(\nabla_1^2 + \nabla_2^2) + \frac{e^2}{4\pi\varepsilon_0}\left(\frac{1}{r_{\alpha\beta}} + \frac{1}{r_{12}} - \frac{1}{r_{1\alpha}} - \frac{1}{r_{1\beta}} - \frac{1}{r_{2\alpha}} - \frac{1}{r_{2\beta}}\right) \quad (2.12)$$

The wave function and energies of a molecule which are found from the Schrödinger equation including the coordinates of electrons (q_i) and nuclei (q_α) is given by:

$$\widehat{H}\psi(q_i, q_\alpha) = E\psi(q_i, q_\alpha) \quad (2.13)$$

Nuclei are much heavier than electrons and so electrons move much faster than nuclei with the same kinetic energy. Hence, to a good approximation as far as electrons are concerned, they can essentially instantly adjust to nuclear motion, and the nuclei positions are fixed. Omitting nuclear kinetic-energy terms gives the Schrödinger equation for electronic motion as:

$$\left(\widehat{H}_{el} + V_{NN}\right)\psi_{el} = U\psi_{el} \quad (2.14)$$

Where the purely electronic Hamiltonian $\widehat{H}_{el}$ is

$$\widehat{H}_{el} = -\frac{\hbar^2}{2m_e}\sum_i \nabla_i^2 + \sum_i \sum_{j>i} \frac{e^2}{4\pi\varepsilon_0 r_{ij}} - \sum_\alpha \sum_i \frac{Z_\alpha e^2}{4\pi\varepsilon_0 r_{i\alpha}} \quad (2.15)$$

The electronic Hamiltonian including nuclear repulsion is $\widehat{H}_{el} + V_{NN}$.

$$V_{NN} = \sum_{\alpha} \sum_{\beta>\alpha} \frac{Z_\alpha Z_\beta e^2}{4\pi\varepsilon_0 r_{\alpha\beta}} \quad (2.16)$$

The energy, U, in Equation 2.14 is the electronic energy including internuclear repulsion. There are an infinite number of possible nuclear configurations, and for each of these we can solve the electronic Schrödinger Equation 2.14 to get a set of electronic wave functions and corresponding energies. The electronic wave functions and energies thus depend parametrically on the nuclear coordinates:

$$\psi_{el} = \psi_{el,n}(q_i; q_\alpha) \quad (2.17)$$

$$U = U_n(q_\alpha) \quad (2.18)$$

where *n* symbolizes the electronic quantum numbers. If V_{NN} is removed from Equation 2.14 we get:

$$\hat{H}_{el}\psi_{el} = E_{el}\psi_{el} \quad (2.19)$$

The electronic energy E_{el} is related to U by:

$$U = E_{el} + V_{NN} \quad (2.20)$$

The electrons act like springs connecting the nuclei. As the internuclear distance changes, the energy stored in the spring changes. Hence the Schrödinger equation for nuclear motion is given by

$$\hat{H}_N\psi_N = E\psi_N \quad (2.21)$$

$$\hat{H}_N = -\frac{\hbar^2}{2}\sum_{\alpha}\frac{1}{m_\alpha}\nabla_\alpha^2 + U(q_\alpha) \quad (2.22)$$

The major assumption of the Born-Oppenheimer approximation is that nuclear and electronic motions are separable. Born-Oppenheimer's mathematical treatment indicates that the true molecular wave function is adequately approximated as

$$\psi(q_i, q_\alpha) = \psi_{el}(q_i; q_\alpha)\psi_N(q_\alpha) \tag{2.23}$$

This approximation yields reasonable results for ground electronic states of diatomic molecules.

Variational Method

The variational theorem states that the energy determined from any approximate wave function will always be greater than the energy for the exact wave function. The variational theorem allows us to calculate an upper bound for a system's ground state energy. It approximates the ground-state energy of a system without having to solve the Schrödinger equation which is based on the equation below

$$\frac{\int \phi^* \hat{H} \phi d\tau}{\int \phi^* \phi d\tau} \geq E_1 \tag{2.24}$$

Where ϕ is a trial variation function and E_1 is the ground state energy.

Perturbation Theory

The time-independent Hamiltonian operator $\hat{H}$ system which cannot solve the Schrödinger equation for the eigenfunctions and eigenvalues of the bound stationary states of a perturbed system is given as

$$\hat{H}\psi_n = E_n\psi_n \tag{2.25}$$

Perturbation theory approximates an unsolvable Schrödinger equation for a perturbed system by making corrections to a solvable, unperturbed, system. For an unperturbed system a similar but slightly different Hamiltonian $\hat{H}^0$ operates on the wave function $\psi_n^{(0)}$ in the solvable Schrödinger equation

$$\hat{H}^0\psi_n^{(0)} = E_n^{(0)}\psi_n^{(0)} \tag{2.26}$$

The difference between the two systems is the perturbation $\hat{H}'$[53]

$$\hat{H} = \hat{H}^0 + \lambda\hat{H}' \tag{2.27}$$

In Equation 2.26, $E_n^{(0)} and\ \psi_n^{(0)}$ are called the unperturbed energy and unperturbed wave function of the state *n*. The continuous parameter λ linearly varies the amount of perturbation in the system. When λ is zero, we have an unperturbed system. As λ increases, the perturbation grows larger, and at $\lambda = 1$ the perturbation is fully "turned on". Corrections to the wave function and energy can be applied as follows[53]

$$\psi_n = \psi_n^{(0)} + \lambda\psi_n^{(1)} + \lambda^2\psi_n^{(2)} + \cdots + \lambda^k\psi_n^{(k)} + \cdots \tag{2.28}$$

$$E_n = E_n^{(0)} + \lambda E_n^{(1)} + \lambda^2 E_n^{(2)} + \cdots + \lambda^k E_n^{(k)} + \cdots \tag{2.29}$$

where $\psi_n^{(k)}$ and $E_n^{(k)}$ are the kth-order corrections to the wave function and energy. The first and second order corrections to the energy is found by averaging the perturbation $\widehat{H}'$ over the appropriate unperturbed wave function and is given in Dirac or bracket notation as[53]

$$E_n^{(1)} = \langle \psi_n^{(0)} | \widehat{H}' | \psi_n^{(0)} \rangle = \int \psi_n^{(0)*} \widehat{H}' \psi_n^{(0)} d\tau \qquad (2.30)$$

$$E_n^{(2)} = \sum_{m \neq n} \frac{\left| \langle \psi_n^{(0)} | \widehat{H}' | \psi_n^{(0)} \rangle \right|^2}{E_n^{(0)} - E_m^{(0)}} \qquad (2.31)$$

Hartree Self-Consistent Field Method

The Hartree-Fock procedure is the basis for the use of atomic and molecular orbitals in many-electron systems. For smaller systems like hydrogen the exact wave function is known, and the wave functions for helium and lithium are accurately calculated using variation functions that include interelectronic distances. The Hamiltonian operator for an n-electron atom is

$$\widehat{H} = -\frac{\hbar^2}{2m_e} \sum_{i=1}^{n} \nabla_i^2 + \sum_{i=1}^{n-1} \sum_{j=i+1}^{n} \frac{e^2}{4\pi\varepsilon_0 r_{ij}} - \sum_{i=1}^{n} \frac{Ze^2}{4\pi\varepsilon_0 r_i} \qquad (2.32)$$

The first term in the atomic Hamiltonian is the sum of kinetic energy operators performed on *n* electrons. The second term consists of potential energies due to interelectronic repulsions. The third term is comprised of the potential energies due to attractions between n electrons and a nucleus of charge *Ze*. If the interelectronic repulsions terms are ignored as an initial approximation, the Schrödinger equation can be split up into n one-electron equations that are similar to the solvable hydrogen atom equation. The zeroth order wave function then becomes a product of one-electron orbitals[55]

$$\psi^{(0)} = f_1(r_1, \theta_1, \phi_1) f_2(r_2, \theta_2, \phi_2) \dots f_n(r_n, \theta_n, \phi_n) \tag{2.33}$$

$$f = R_{nl}(r) Y_l^m(\theta, \phi) \tag{2.34}$$

$R_{nl}(r)$ are called the radial wave functions[56]

$$R_{nl}(r) = -\left\{\frac{(n-l-1)!}{2n[(n+1)!]^3}\right\}^{1/2} \left(\frac{2}{na_0}\right)^{l+\frac{3}{2}} r^l e^{\frac{-r}{na_0}} L_{n+l}^{2l+1}\left(\frac{2r}{na_0}\right) \tag{2.35}$$

where n and l are the principal and orbital angular momentum quantum numbers, respectively, a_0 is the Bohr radius, and the L_{n+l}^{2l+1} are called the associated Laguerre polynomials. $Y_l^m(\theta, \phi)$ are the spherical harmonics[57]

$$Y_l^m(\theta, \phi) = \left[\frac{2l+1}{4\pi} \frac{(l-|m|)!}{(l+|m|)!}\right]^{1/2} P_l^{|m|}(\cos\theta) e^{im\phi} \tag{2.36}$$

The magnetic quantum number is given by m, where $|m| \leq l$. The $P_l^{|m|}(\cos\theta)$ are called the associated Legendre functions[56]

$$P_l^{|m|}(\cos\theta) = \frac{1}{2^l l!}(1 - cos^2\theta)^{|m|/2} \frac{d^{l+|m|}}{d(\cos\theta)^{l+|m|}} (cos^2\theta - 1)^l, \quad l = 0, 1, 2, \dots$$

(2.37)

The use of different effective nuclear charges for different orbitals can approximate the shielding effect using unrestricted variational functions to any form of orbitals.[56]

$$\phi = g_1(r_1, \theta_1, \phi_1) g_2(r_2, \theta_2, \phi_2) \dots g_n(r_n, \theta_n, \phi_n) \tag{2.38}$$

The functions $g_1, g_2 \ldots g_n$, are varied to minimize Equation 2-24. The Hartree self-consistent-field (SCF) method is a procedure for finding the functions g_i.[58]

Hartree's Procedure

The Hartree method is a single electron approximation technique used in multi-electron systems. The molecular Hamiltonian is split up into individual single electron Hamiltonians. Hartree's procedure is as follows: We first predict a wave function

$$\phi = s_1(r_1, \theta_1, \phi_1)s_2(r_2, \theta_2, \phi_2) \ldots s_n(r_n, \theta_n, \phi_n) \tag{2.39}$$

where s_i is a normalized function of r multiplied by a spherical harmonic. The potential energy between two-point charges q_1 and q_2 is given as

$$V_{12} = \frac{q_1 q_2}{4\pi\varepsilon_0 r_{12}} \tag{2.40}$$

If Electron 2 is marked out into a continuous charge distribution, its infinitesimal charge is $\rho_2 dv_2$ in an infinitesimal volume dv_2, where ρ_2 is the charge density. Substitution of $\rho_2 dv_2$ for q_2 and integration of Equation 2.40 sums up the interactions between Electron 1 and the infinitesimal elements of charge from Electron 2

$$V_{12} = \frac{q_1}{4\pi\varepsilon_0} \int \frac{\rho_2}{r_{12}} dv_2 \tag{2.41}$$

Electrons have a charge of $-e$, so the charge density of Electron 2 is equal to $-e|s_2|^2$, where $|s_2|^2$ is the probability density of Electron 2

$$V_{12} = \frac{e^2}{4\pi\varepsilon_0}\int \frac{|s_2|^2}{r_{12}} dv_2 \qquad (2.42)$$

The interactions between Electron 1 and the remaining $n-1$ electrons are summed to give

$$V_{12} + V_{13} + \cdots + V_{1n} = \sum_{j=2}^{n} \frac{e^2}{4\pi\varepsilon_0}\int \frac{|s_j|^2}{r_{1j}} dv_j \qquad (2.43)$$

Therefore, the potential energy of the interactions of Electron 1 with the $n-1$ electrons and the nucleus is given as

$$V_1(r_1, \theta_1, \phi_1) = \sum_{j=2}^{n} \frac{e^2}{4\pi\varepsilon_0}\int \frac{|s_j|^2}{r_{1j}} dv_j - \frac{Ze^2}{4\pi\varepsilon_0 r_1} \qquad (2.44)$$

The central-field approximation averages $V_1(r_1, \theta_1, \phi_1)$ over the angles θ_1 and ϕ_1 to reduce the potential energy to a spherically symmetric function $V_1(r_1)$ that depends only on r_1.

$$V_1(r_1) = \frac{\int_0^{2\pi}\int_0^{\pi} V_1(r_1,\theta_1,\phi_1)\sin\theta d\theta_1 d\phi_1}{\int_0^{2\pi}\int_0^{\pi}\sin\theta d\theta d\phi} \qquad (2.45)$$

$V_1(r_1)$ is then incorporated into the one-electron Schrödinger equation as the potential energy term

$$\left[-\frac{\hbar^2}{2m_e}\nabla_1^2 + V_1(r_1)\right] t_1(1) = \varepsilon_1 t_1(1) \qquad (2.46)$$

$t_1(1)$ is an improved orbital for Electron 1 and ε_1 is the energy of the orbital. The sum of orbital energies is not the energy of the system because it doubly includes all interelectronic repulsions. Therefore, the total energy of the system is calculated by

subtracting the average repulsions of electrons in orbitals from the sum of the orbital energies ε_i.

$$E = \sum_{i=1}^{n} \varepsilon_i - \sum_{i=1}^{n-1} \sum_{j=i+1}^{n} \iint \frac{e^2 |g_i(i)|^2 |g_j(j)|^2}{4\pi\varepsilon_0 r_{ij}} dv_i dv_j \qquad (2.47)$$

The Wave Function as a Slater Determinant

The Hartree-Fock (HF) wave function is written as anti-symmetrized and normalized products of spin orbitals. Hartree's procedure uses spatial orbitals that do not explicitly include spin and the antisymmetrical property of the interchange of electrons. An antisymmetrized spin-orbital incorporates these properties of electrons by being comprised of a spatial orbital and a spin function. The differential equation for the Hartree-Fock calculation is:[59]

$$\hat{F} u_i = \varepsilon_i u_i, \quad i = 1, 2, \ldots, n \qquad (2.48)$$

where $\hat{F}$ is the Fock operator, u_i is a spin-orbital with orbital energy ε_i. Equation 2-48 only works for a wave function that can be written as a single Slater determinant. The properties of Slater determinants satisfy the antisymmetry property of electron systems.[60] A wave function can be represented by a Slater determinant or a linear combination of Slater determinants, where the column elements of a single column involve the same spin-orbital, and the row elements of a single row involve the same electron. The ground-state of the zeroth-order helium can be rewritten as the following Slater determinant[60]

$$1s(1)1s(2) \cdot \frac{1}{\sqrt{2}}[\alpha(1)\beta(2) - \beta(1)\alpha(2)] = \frac{1}{\sqrt{2}} \begin{vmatrix} 1s(1)\alpha(1) & 1s(1)\beta(1) \\ 1s(2)\alpha(2) & 1s(2)\beta(2) \end{vmatrix} \qquad (2.49)$$

The general properties of the Slater determinant with the perspective of the present context can be summarized as follows, it allows only antisymmetric electronic exchange within

an orbital, two electrons present in an orbital should have opposite spin. If the spins were identical, then the Slater determinant would be: Equation 2.49 which on simplifying, we get zero. Hence, the Slater determinant wavefunction vanishes if the electrons have identical spin. The wavefunction set according to Pauli's exclusion principle is said to be antisymmetrized and molecular orbital is obtained by the linear combination of atomic orbitals (LCAO). Hence, it is possible to have an approximation of molecular orbitals by considering them as made out of linear combination of antisymmetrized determinantal wavefunctions. Columns are one-electron wavefunctions molecular orbitals. Rows contain the electron coordinates.

Two commonly used Hartree-Fock SCF methods for open-shell systems are the restricted open-shell Hartree-Fock (ROHF) and the unrestricted Hartree-Fock (UHF) methods.[61] The SCF energy of the closed-subshell configuration for the atomic ^{1}S term is given as

$$E = \langle D|\widehat{H}_{el}|D\rangle = 2\sum_{i=1}^{\frac{n}{2}}\langle\phi_i(1)|\hat{f}_1|\phi_i(1)\rangle + \sum_{j=1}^{\frac{n}{2}}\sum_{i=1}^{\frac{n}{2}}(2J_{ij} - K_{ij}) \qquad (2.50)$$

where ϕ_i are the $\frac{n}{2}$ spatial orbitals for n electrons and D is the Slater determinant Hartree-Fock wave function of orthonormal spin-orbitals u is given as

$$D = \frac{1}{\sqrt{n!}}\begin{vmatrix} u_1(1) & \dots & u_n(1) \\ \vdots & \ddots & \vdots \\ u_1(n) & \dots & u_n(n) \end{vmatrix} \qquad (2.51)$$

Where spin-orbital $u_i = \theta_i\sigma_i$, θ_i is a spatial orbital and σ_i is a spin function. J_{ij} and K_{ij} are the Coulomb and exchange integrals, respectively.

$$J_{ij} = \left\langle \phi_i(1)\phi_j(2)\left|\frac{1}{r_{12}}\right|\phi_i(1)\phi_j(2)\right\rangle \qquad (2.52)$$

$$K_{ij} = \left\langle \phi_i(1)\phi_j(2) \middle| \frac{1}{r_{12}} \middle| \phi_j(1)\phi_i(2) \right\rangle \tag{2.52}$$

The molecular electronic Hamiltonian is written as

$$\hat{H}_{el} = \sum_{i=1}^{n} \hat{f}_i + \sum_{i=1}^{n-1} \sum_{j>i} \hat{g}_{ij} \tag{2.53}$$

$\hat{f}_i$ and $\hat{g}_{ij}$ are the one-electron and two-electron operators, respectively, which are defined in atomic units as

$$\hat{f}_i = -\frac{1}{2}\nabla_i^2 - \sum_{\alpha} \frac{Z_\alpha}{r_{i\alpha}} \tag{2.54}$$

$$\hat{g}_{ij} = \frac{1}{r_{ij}} \tag{2.55}$$

Equation 2.50 is slightly modified to give the Hartree-Fock energy of a polyatomic molecule or a closed-shell diatomic.

$$E_{HF} = \langle D \middle| \hat{H}_{el} + V_{NN} \middle| D \rangle \tag{2.56}$$

$$E_{HF} = 2\sum_{i=1}^{\frac{n}{2}} H_{ii}^{core} + \sum_{j=1}^{\frac{n}{2}} \sum_{i=1}^{\frac{n}{2}} \left(2J_{ij} - K_{ij}\right) + V_{NN} \tag{2.57}$$

$\hat{H}^{core}$ is the one-electron core Hamiltonian

$$H_{ii}^{core} = \left\langle \phi_i(1) \middle| \hat{H}^{core}(1) \middle| \phi_i(1) \right\rangle = \left\langle \phi_i(1) \middle| -\frac{1}{2}\nabla_i^2 - \sum_{\alpha} \frac{Z_\alpha}{r_{i\alpha}} \middle| \phi_i(1) \right\rangle \tag{2.58}$$

The Hartree-Fock method finds molecular orbitals (MOs) ϕ_i that minimize the variational integral E_{HF}.[62] The differential equation for the Hartree-Fock operation on the MOs is

$$\hat{F}(1)\phi_i(1) = \varepsilon_i\phi_i(1) \tag{2.59}$$

Where the ε_i are the orbital energies and $\hat{F}$ is the Hartree-Fock operator also defined as

$$\hat{F}(1) = \hat{H}^{core}(1) + \sum_{j=1}^{\frac{n}{2}}\left[2\hat{J}_j(1) - \hat{K}_j(1)\right] \tag{2.60}$$

$\hat{J}_j$ and $\hat{K}_j$ are the Coulomb and exchange operators, respectively.

$$\hat{J}_j(1)f(1) = f(1)\int\left|\phi_j(2)\right|^2\frac{1}{r_{12}}dv_2 \tag{2.61}$$

$$\hat{K}_j(1)f(1) = \phi_j(1)\int\frac{\phi_j^*(2)f(2)}{r_{12}}dv_2 \tag{2.62}$$

The orbital energies are calculated by multiplying Equation 2.59 by ϕ_i^* to obtain Equations 2.63 and 2.64

$$\varepsilon_i = \left\langle\phi_i(1)\middle|\hat{H}^{core}(1)\middle|\phi_i(1)\right\rangle + \sum_j\left[2\left\langle\phi_i(1)\middle|\hat{J}_j(1)\middle|\phi_i(1)\right\rangle - \left\langle\phi_i(1)\middle|\hat{K}_j(1)\middle|\phi_i(1)\right\rangle\right] \tag{2.63}$$

$$\varepsilon_i = H_{ii}^{core} + \sum_{j=1}^{\frac{n}{2}}\left(2J_{ij} - K_{ij}\right) \tag{2.64}$$

Summing over *n* divided by 2 occupied orbitals results in

$$\sum_{i=1}^{\frac{n}{2}}\varepsilon_i = \sum_{i=1}^{\frac{n}{2}}H_{ii}^{core} + \sum_{j=1}^{\frac{n}{2}}\sum_{i=1}^{\frac{n}{2}}\left(2J_{ij} - K_{ij}\right) \tag{2.65}$$

The Hartree-Fock energy then is obtained by substituting the solution for $\sum_i H_{ii}^{core}$ from Equation 2.65 into Equation 2.57

$$E_{HF} = 2\sum_{i=1}^{\frac{n}{2}}\varepsilon_i - \sum_{j=1}^{\frac{n}{2}}\sum_{i=1}^{\frac{n}{2}}\left(2J_{ij} - K_{ij}\right) + V_{NN} \tag{2.66}$$

where the factor of 2 accounts for two electrons within each spatial orbital.

Roothaan and Hall Equations

Roothaan-Hall equations are obtained by extending the concepts of the variational principle and the linear combination of atomic orbitals (LCAOs) to the HF equation.[63] The Hartree Fock equation can, in principle be solved by any standard method for solving integro-differential equations. For atoms, solutions of the HF equations reaching the HF limit is routine and can be carried out by numerical integration. However, for large molecules, solutions reaching the HF limit are not possible. In fact, the HF procedure leads to a complicated set of near-intractable, integro-differential equations, which can only be solved with any ease for a one-center problem. The Roothaan equations are a representation of the Hartree-Fock equation in a non-orthonormal basis set which can be of Gaussian type or Slater-type.[64] It applies to closed-shell molecules or atoms where all molecular orbitals or atomic orbitals, respectively, are doubly occupied.[64] This is generally called Restricted Hartree–Fock theory. The method was developed independently by Clement C. J. Roothaan and George G. Hall in 1951 and is thus sometimes called the Roothaan-Hall equations.[64, 65] The Roothaan-Hall equations can be written in a form resembling a generalized eigenvalue problem, although they are not a standard eigenvalue problem because they are nonlinear: Roothaan proposed that Hartree-Fock orbitals could be represented by linear combinations of a set of known functions called basis functions. Denoting the atomic orbital basis functions as χ_s, we have the expansion

$$\phi_i = \sum_{s=1}^{b} c_{si}\chi_s \qquad (2.67)$$

Where c_{si} are the expansion coefficients and χ_s is a set of one-electron basis functions. As the energy is minimized, the coefficients, c_{si} , will be optimized, while the basis functions remain unchanged. Although any sets of mathematically-suitable functions which spans the

space of electron distribution could be used as basis functions, the concept of molecular orbitals as linear combination of atomic orbitals (LCAO-MO) have proved to be very useful. Moreover, each spin orbital can be described by more than just one basis function. Substituting Roothaan's orbital expansion into Equation into 2.59 gives

$$\sum_s c_{si}\hat{F}\chi_s = \varepsilon_i \sum_s c_{si}\chi_s \tag{2.68}$$

Left multiplying by χ_r^* and integrating yields a linear homogenous equation that describe a MO.

$$\sum_{s=1}^{b} c_{si}(F_{rs} - \varepsilon_i S_{rs}) = 0, \quad r = 1, 2, \dots, b \tag{2.69}$$

Or even more simply as matrices

$$\det(F_{rs} - \varepsilon_i S_{rs}) = 0 \tag{2.70}$$

where ε is a diagonal matrix of the orbital energies ε_i . This is like an eigenvalue equation except for the overlap matrix S_{rs}. One performs a transformation of basis to go to an orthogonal basis to make S_{rs} vanish. Then it's just a matter of solving an eigenvalue equation. Since F_{rs} depends on its own solution (through the orbitals), the process must be done iteratively.

Restricted and Unrestricted Hartree-Fock Methods

The setting up of the HF model by imposing the double occupancy principle is called the Restricted Hartree-Fock (RHF) model. For an open-shell system orbital, pairing does not occur in any level of computation.[63] There are two possibilities for extending HF calculations to open-shell systems: first strictly presuming that orbital pairing does not occur in any level. Each spin orbital is allowed to have its own spatial part. This type of modeling is known as Unrestricted Hartree-Fock (UHF) modeling. Second, the RHF procedure is extended to spatial orbitals other

than the orbitals which are singly occupied. Modeling of this type is known as restricted open shell Hartree-Fock modeling (ROHF).

In UHF, V_{HF}^{α} and V_{HF}^{β} orbitals will have different effective potentials. UHF affords equations which are much simpler than that of ROHF. In UHF, wavefunctions are composed of single Slater determinants, while in ROHF, wavefunctions are composed of the linear combination of a few determinants, where the expansion coefficients are decided by the symmetry of the state. However, the UHF Slater determinant is not an eigenfunction of the total spin operator $\hat{S}^2$. The expectation value of spin $< \hat{S}^2 >$ may be deviated from the actual value S(S + 1), where S is the spin quantum number corresponding to the total spin of the system. The more the deviation, the more will be the contamination in the determinant with functions corresponding to states of higher spin multiplicity. Hence, in computational practice, the UHF approach may not be convenient. For RHF/ROHF, α and β spins have the same spatial part. Here, the wavefunction is an eigenfunction of the $\hat{S}^2$ operator. For open-shell systems, the unpaired electron interacts differently with α and β spins. The optimum spatial orbitals are different. Restricted formalism is not suitable for spin dependent properties. For UHF, α and β spins have different spatial parts. The wavefunction is not an eigenfunction of the $\hat{S}^2$ function and may be deviated with states of higher multiplicity (2S +1). It yields qualitatively correct spin densities. Energy computed by UHF-method will be less than or equal to energy computed by the RHF or ROHF methods, i.e., E(UHF) ≤ E(RHF). HF methods are the starting point for more advanced calculations that include electron correlation.

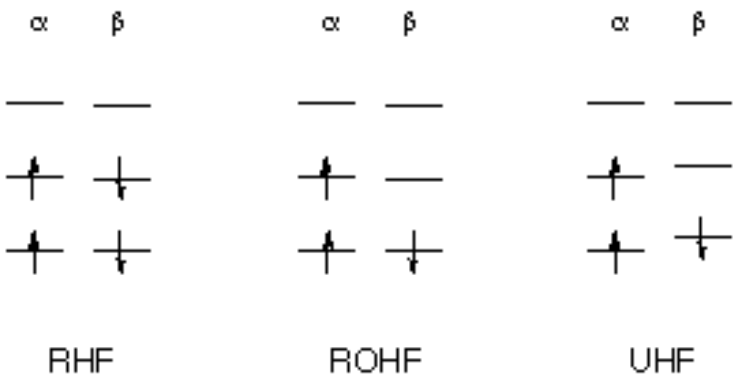

Figure 12: Comparison of computed energy with different types of HF calculation

While UHF calculations on open shell systems usually give lower energies and a better description of the unpaired electron density distribution (and thus EPR spectra), the UHF wavefunction is not an eigenfunction of the $< \hat{S}^2 >$ operator. In particular for spin-delocalized systems such as allylic or benzylic radicals, the UHF wavefunction can deviate substantially from that for a doublet state. The degree of deviation can be characterized through the difference between the expectation value of the $< \hat{S}^2 >$ operator (given after the SCF convergence note in the output file) and the value of S(S+1) for the current spin quantum number of the system.

Density Functional Theory

The electronic wave function of an *n*-electron molecule depends on *3n* spatial and *n* spin coordinates. Since the Hamiltonian operator contains only one-electron and two-electron spatial terms, it is found that the molecular energy can be written in terms of integrals involving only six spatial coordinates, this implies that the wave function of a many-electron molecule contains more information than is required making it lack direct physical significance. This led to a search for functions that involve fewer variables than the wave function which can also be used to calculate the energy and other properties of the molecule. The basic principle of Density Functional Theory (DFT) is that the energy of the molecule may be determined from the electron

density instead of the approximate many electron wave function.[66] The current DFT method originated from the Hohenberg-Kohn theorem,[67] which states that all properties of a system defined by an external potential are uniquely determined by the ground state electron density. Hence the state of the electron density that gives the minimum total energy is the ground state electron density.[66] The functional E_{xc} can be written as the sum of the exchange energy functional E_x and correlation-energy functional E_c as an aid to developing functionals in Kohn-Sham (KS) DFT[68]

$$E_{xc} = E_x + E_c \tag{2.71}$$

E_x can be defined by the same formula used for the exchange energy in Equation 2.57 that involve the exchange integrals K_{ij} defined in Equation 2.52 by replacing the Hartree-Fock orbitals with Kohn-Sham orbitals

$$E_x \equiv -\frac{1}{4}\sum_{i=1}^{n}\sum_{j=1}^{n}\left\langle \theta_i^{KS}(1)\theta_j^{KS}(2)\left|\frac{1}{r_{12}}\right|\theta_j^{KS}(1)\theta_i^{KS}(2)\right\rangle \tag{2.72}$$

The factor ¼ accounts for the fact that in Equation 2.57 we are summing over the orbitals whereas in Equation 2.68 we are summing over the electrons. The correlation-energy functional E_c is then found by subtracting E_x from E_{xc}. While E_x can be evaluated using Equation 2.68, approximation of both E_x and E_c using a model such as the Local Density Approximation (LDA) tends to produce error cancellation and more accurate results.

Hohenberg and Kohn used the LDA model to assume that if the electron density ρ varies negligibly with position, then $E_x^{LDA}[\rho]$ is accurately given by Equation 2.69 resulting in the exchange-correlation functional[67]

$$E_x^{LDA}[\rho] = \int \rho(r)\varepsilon_{xc}(\rho)dr \tag{2.73}$$

where $\varepsilon_{xc}(\rho)$ is the exchange plus correlation energy per electron in a homogeneous electron gas of electron density ρ. The Local-Spin-Density Approximation (LSDA) model for open-shell systems is like the UHF method by allowing different spatial Hartree-Fock orbitals for electrons with different spins.[58] The electron density's dependence on position must be included in order to improve on the LDA and LSDA models. The Gradient-Corrected (GGA) functionals incorporate this dependency by including the gradients of the electron densities ρ^α and ρ^β of the paired electrons[69]

$$E_{xc}^{GGA}\left[\rho^\alpha, \rho^\beta\right] = \int f\left(\rho^\alpha(r), \rho^\beta(r), \nabla\rho^\alpha(r), \nabla\rho^\beta(r)\right) dr \tag{2.74}$$

where E_{xc}^{GGA} can be separated into the sum of exchange and correlation functionals similar to Equation 2-67. The Becke's 1988 exchange functional is a gradient correction to the E_x^{LSDA} and is given as**Error! Bookmark not defined.**

$$E_x^{B88} = E_x^{LSDA} - b\sum_{\sigma=\alpha,\beta}\int \frac{(\rho^\sigma)^{\frac{4}{3}}\chi_\sigma^2}{1+6b\chi_\sigma \ln\left[\chi_\sigma+(\chi_\sigma^2+1)^{\frac{1}{2}}\right]} dr = E_x^{LSDA} + \Delta E_x^{B88} \tag{2.75}$$

where b is an empirical parameter whose value in atomic units is determined by fitting known Hartree-Fock exchange energies to several atoms, χ_σ is equivalent to $|\nabla\rho^\sigma|/(\rho^\sigma)^{4/3}$, and E_x^{LSDA} is defined as:[69]

$$E_x^{LSDA} = -\frac{3}{4}\left(\frac{6}{\pi}\right)^{1/3}\int\left[(\rho^\alpha)^{4/3} + (\rho^\beta)^{4/3}\right]dr \tag{2.76}$$

The use of a hybrid exchange-correlation functional B3PW91 was first proposed by Becke, and it incorporated both Equation 2.68 and GGA exchange and correlation functionals.[70] The three-parameter functional Becke3LYP or B3LYP was therefore named after Becke and is defined as[70]

$$E_{xc}^{B3LYP} = (1 - a_0 - a_x)E_x^{LSDA} + a_0E_x^{HF} + a_xE_x^{B88} + (1 - a_c)E_c^{VWN} + a_cE_c^{LYP} \quad (2.77)$$

The parameters a_0, a_x, and a_c are chosen to give fits to experimental molecular atomization energies

Basis Sets

A basis set is a mathematical description of orbitals of a system, which is used for approximate theoretical calculations or modeling. All the modern theories previously described begin calculations with basis set functions. In computational chemistry, basis sets are composed of nonorthogonal, one-electron functions called atomic orbitals that are used to build molecular orbitals. The two most common basis function types are Slater-type orbitals and the Gaussian-type orbital. It is a set of basic functional building blocks that can be stacked or added to have the features that are needed. By "stacking" in mathematics, it's meant adding things, possibly after multiplying each of them by its own constant:

$$\psi = a_1\phi_1 + a_2\phi_2 + \cdots + a_k\phi_k \quad (2.78)$$

where k is the size of the basis set, $\phi_1, \phi_2, ..., \phi_k$ are the basis functions and $a_1, a_2, ..., \phi_k$ are the normalization constants. It was John C. Slater who first turned to orbital computation using basis sets, known as Slater Type Orbitals (STOs). The solution of the Schrödinger equation for

the hydrogen atom and other one-electron ions gives atomic orbitals which are a product of a radial function that depend on the distance of the electron from the nucleus and a spherical harmonic. He pointed out that one could use functions that consisted only of the spherical harmonics and the exponential term. Slater-type orbitals represent the real situation for the electron density in the valence region and beyond but are not so good nearer to the nucleus. Strictly speaking, atomic orbitals (AOs) are the real solutions of the Hartree-Fock (HF) equations for the atom, i.e., wavefunctions for a single electron in the atom. Anything else is not really an atomic orbital function. Hence these functions are named as "basis functions" or "contractions," which are more appropriate. Earlier, the STOs were used as basis functions due to their similarity to atomic orbitals of the hydrogen atom. Many calculations over the years have been carried out with STOs, particularly for diatomic molecules. Slater fits linear least-squares to data that could be easily calculated. The general expression for a basis function[71] is given in Equation 2.79

$$\text{Basis function, } BF = N \times e^{(-\alpha r)} \tag{2.79}$$

where N is the normalization constant, α is the orbital exponent and r is the radius in angstroms. STOs are described by the function depending on spherical coordinates:[63]

$$\phi_1 = (\alpha, n, l, m; r, \theta\ \phi) = N r^{n-1} e^{-\alpha r} Y_{l,m}(\theta\ \phi) \tag{2.80}$$

The r, θ and ϕ are spherical coordinates, and $Y_{l,m}$ is the angular momentum part (the function describing the "shape"). The n, l and m are quantum numbers: principal, angular momentum, and magnetic, respectively. Simplifying the equation for hydrogen-like systems, the STO equation takes the form of:[63]

$$STO = [\frac{\alpha^3}{\pi}]^{0.5} e^{(-\alpha r)} \tag{2.81}$$

where α is the Slater orbital exponent. STOs are approximate solutions to the eigenvalue equation, represented by Equation 2.78

In the 1950s, Frank Boys from Cambridge University in the UK suggested a modification to the wavefunction by introducing Gaussian type functions,[72] which contain the exponential $e^{-\beta r^2}$, rather than the $e^{-\alpha r}$ of the STOs. Such functions are very easy to evaluate. These functions neither represent the electron density of the real situation (the square of a wavefunction is a measure of electron density) nor the STOs. But we can overcome this difficulty to a large extent by using more Gaussian-type orbitals (GTOs). Some early calculations used a large number of individual GTOs. It was then suggested that the GTOs be contracted into separate functions. Each basis function in this approach consists of several GTOs combined together in a linear manner with fixed coefficients. Thus, we might define a GTO (3G) basis function as:[73,74,75]

$$GTO(3G) = c_1 e^{-\beta_1 r^2} + c_2 e^{-\beta_2 r^2} + c_3 e^{-\beta_3 r^2} \qquad (2.82)$$

where the three values of c and β are fixed, and that number is included in the designation. The values of the c and β can be found in several ways. One common way is to fit the above expression to a STO using a least squares method. Other methods involve varying them in atomic calculations to minimize the energy. Expansions of any number of GTOs are possible, but usually less than six are used due to computational reasons. Treating Gaussians as GTOs is probably a misnomer, since they are not really orbitals. They are modified and simplified forms of functions. In recent literature, they are frequently called Gaussian primitives. A Cartesian Gaussian centered on atom *a* can be represented as:

$$G_{i,j,k} = N x_a^i y_a^j k_a^k e^{-\alpha r_a^2} \qquad (2.83)$$

where *i, j,* and *k* are nonnegative integers, α is a positive orbital exponent,x_a,y_a and z_a are Cartesian coordinates with the origin at *a,* and N is the Cartesian Gaussian normalization constant. This constant is given by the expression:

$$N = \left(\frac{2\alpha}{\pi}\right)^{\frac{3}{4}} \left[\frac{(8\alpha)^{i+j+k} i!\, j!\, k!}{(2i)!(2j)!(2k)!}\right]^{\frac{1}{2}} \qquad (2.84)$$

when $i = 0$, $j = 0$, $k = 0$ and $i + j + k = 0$, then the Gaussian type function (GTF) is known as the *s*-type function; when $i + j + k = 1$, we have a *p*-type function, when $i + j + k = 2$,, we have the *d*-type function, and so on. There are six possible *d*-Gaussian functions. These *d*-functions can be modified into five linear combinations, to have the same angular behavior as the real *3d* atomic orbitals.

Basis sets can be broadly classified into the following types. Minimal basis sets: STO-3G, STO-4G, STO-6G, STO-3G* – a polarized version of STO-3G. Pople basis sets: 3-21g, 3-21g* – Polarized, 3-21+g – Diffuse, 3-21+g* – With polarization and diffuse functions, 6-31g, 6-31g*, 6-31+g*, 6-31g (3df, 3pd),6- 311g, 6-311g*, 6-311+g*.[63] Correlation consistent basis sets: These basis sets are used for post HF calculations. They include shells of polarization (correlating) functions (d, f, g, etc.) that can yield convergence of the electronic energy to the complete basis set limit. Examples of these are cc-pVDZ (correlation consistent valence double zeta) cc-pVTZ (correlation consistent valence triple zeta) cc-pVQZ (correlation consistent valence quadruple zeta), cc-pV5Z (correlation consistent valence quintuple zeta), aug-cc-pVDZ (Augmented versions of cc-pVDZ), etc.[63] Other split valence basis sets: (They have generic names), such as SV(P), SVP, DZV, TZV, TZVPP, or valence triple-zeta plus polarization, QZVPP, valence quadruple-zeta plus polarization.[63] Double, triple, and quadruple zeta basis sets: Basis sets in which there are multiple basis functions corresponding to each atomic orbital, including both valence orbitals and inner orbitals, which are called zeta basis sets. The most common is the D95 basis set of Dunning.[76,77] Plane wave basis sets: In addition to localized basis sets, plane wave basis sets can also be used in quantum chemical simulations. Typically, a finite

number of plane wavefunctions are used, below a specific cutoff energy which is chosen for a certain calculation. These basis sets are popular in calculations.

Atomic Units

Atomic units form a system of natural units which is used for calculations. The results of accurate quantum-mechanical calculations on atoms and molecules are obtained using atomic units. Quantum chemists use atomic units to simplify calculations. They are based on gaussian units in which the fundamental natural constants are the charge on a proton (e), the mass of an electron (m_e), and the reduced Planck's constant ($\hbar$). The base units are set to a value of 1. The unit of permittivity is set to $4\pi\varepsilon_0$, where ε_0 is the permittivity of vacuum. The atomic unit of energy is called the Hartree (E_h):

$$1\ hartree \equiv E_h \equiv \frac{m_e e^4}{(4\pi\varepsilon_0)^2\hbar^2} = 27.211\ eV = 4.3597 \times 10^{-18}\ J \qquad (2.85)$$

The atomic unit of length is the Bohr radius and is equivalent to the length of the radius of the first Bohr orbit in the Bohr model of the hydrogen atom.

$$1\ bohr \equiv a_0 \equiv \frac{4\pi\varepsilon_0\hbar^2}{m_e e^2} = 0.52918\ \text{Å} = 5.2918 \times 10^{-11}\ m \qquad (2.86)$$

The advantage of using atomic units is that it brings the electronic Schrödinger equation to its intrinsically simple form such that the key atomic properties will have the values of 1 as shown[78]

$$\widehat{H} = -\frac{1}{2}\left(\nabla_\alpha^2 + \nabla_\beta^2\right) - \frac{1}{2}(\nabla_1^2 + \nabla_2^2) + \frac{1}{r_{\alpha\beta}} + \frac{1}{r_{12}} - \frac{1}{r_{1\alpha}} - \frac{1}{r_{1\beta}} - \frac{1}{r_{2\alpha}} - \frac{1}{r_{2\beta}} \qquad (2.87)$$

CHAPTER 3

RESULTS AND DISCUSSION

Computational Details

The interactions between four amino acids residues and the guanine radical cation were investigated by B3LYP functional[70] and DFT[66] approach. These model groups were used to stimulate interactions between the amino acids active side-chain groups and the guanine radical cation. All geometries were optimized at the B3LYP/6-31+G (d,p)[69] level of theory. The transition-states were characterized by one imaginary frequency. All calculations were carried out using the Guassian 09 program package version 09.D.01.[79] The enegies for the reactants, transition and product the optimised geometries were determined using the Gaussian 09 program version 09.D.01. The formcheck and cubegen utilities were used for formatting and spin density visualizations respectivetly. Most of these calculations were carried out by Extreme Science and Engineering Discovery (XSEDE) organization and the rest on an eight core HP computer using Linux program. The potential energy curves were plotted from the calculated energies using a spreadsheet (Excel 2016)

Model

Because this work focused on genomic DNA, in the presence of histone, 9-methylguanine with a nearby amino acid side chains were modeled, and the amino acid side chains do not interact with the part of guanine that is involved in the Watson-Crick base-pairing. Again since this work focused on a physiological pH, with pKa 3.9, the N1-H on guanine had been removed.

Discussion of Results

It is reported that reduction of the oxidized guanine in plasmid DNA contains the transfer of an electron as well as proton.[80] For the amino acid-base complexes considered here, it is interesting that after one-electron oxidation histidine and tryptophan side chain guanine complex, a hole is trapped at both the amino acid and guanine moieties, and with the transfer of a proton from the amino acid to the guanine moiety, the hole almost entirely localizes on the amino acid. In other words, when a proton transfers to guanine, the hole is no longer trapped at the guanine but at the amino acid moiety. From the optimised structures of the reactant, transition state and product state complexes the energies were calculated in hartrees (E_h), 1 Hartree = 2625.500 kJ/mol. At the transition state a proton lies in the middle of the amino acids moiety and the guanine radical cation moiety. The energy barrier of these complexes were calculated to be 0.0070 E_h, 0.0113 E_h, 0.0065 E_h, 0.0037 E_h for cysteine, histidine, tyrosine, and tryptophan side chains respectively. The observed **single imaginary frequencies** for the **transition state complexes were** 1316.5764 cm^{-1},1433.6993 cm^{-1},1352.8521 cm^{-1},1186.9687 cm^{-1} for cysteine, histidine, tyrosine, and tryptophan side chain respectively. Figure 13 shows cysteine side chain and guanine complex before electron transfer coupled with proton transfer with Figure 13a showing atoms and Figure 13b showing spin densities

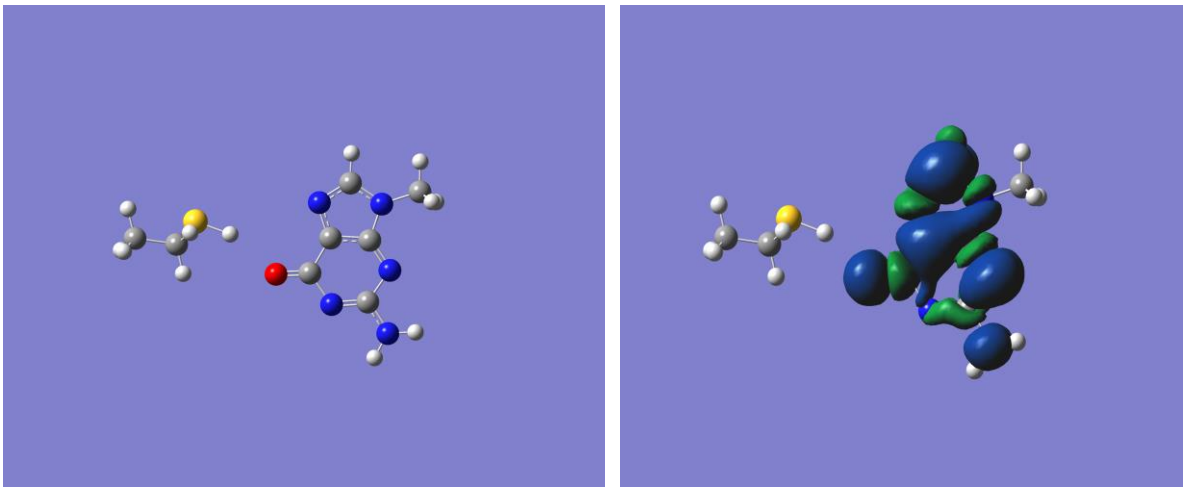

a **b**

Figure 13: Cysteine side chain and guanine complex before electron transfer coupled with proton transfer with (a) showing atoms and (b) showing spin densities

In Figure 13b, before the oxidation of cysteine, all the spin densities were located on guanine radical cation moiety, indication that a hole is located on the guanine radical cation. Figures 14a and Figure 14b show cysteine and guanine radical cation electron transfer coupled with proton transfer to guanine radical cation at the transition state

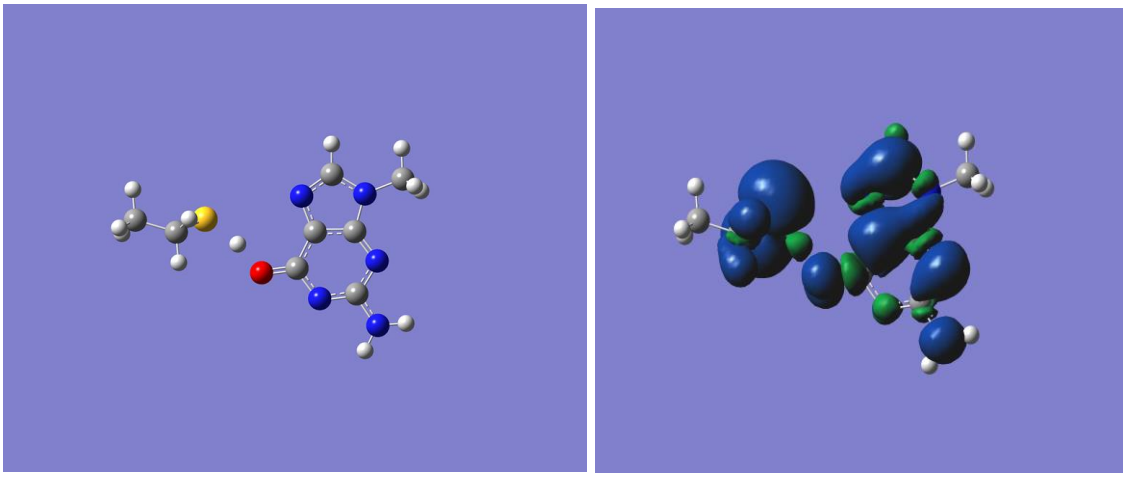

a **b**

Figure 14: Cysteine side chain and guanine radical cation complex showing electron transfer coupled with proton transfer to guanine radical cation at the transition state

At the transition state a proton lies in the middle of the cysteine amino acids moiety and the guanine radical cation moiety. It is observed that the spin densities begins to migrate to the cysteine amino acid moiety in Figure 14b. At the product state all the spin densities migrated to the cysteine amino acid moiety indicating a complete transter of hole to the cysteine amino acid. Figure 15 shows cysteine amino acid with guanine radical cation after electron transfer coupled with proton trasfer at the product state.

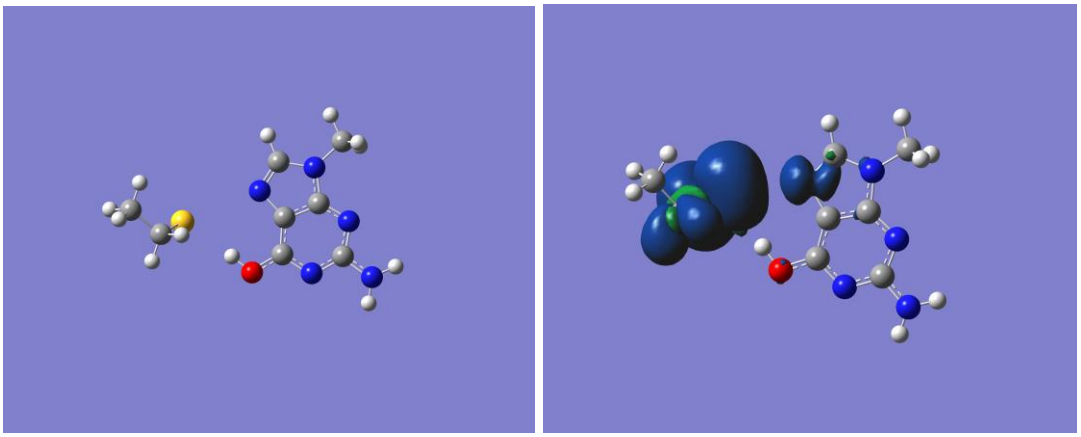

a **b**

Figure 15: Cysteine side chain with guanine radical cation after electron transfer coupled with proton trasfer at the product state

The energies at various state were calculated from the Gaussian 09 program and tableted in Table 3 below

Table 3: Calculated energies at the various state of the cysteine side chain and guanine radical cation complexes.

Cysteinyl and guanyl complexes	Energies / E_h
Reactant	-1059.2747
Transition state	-1059.2677
Product	-1059.2957

The potential energy curve along the cysteinyl (S-H-O) guanyl coordinate was obtained by plotting the cysteine side chain and guanine complexes of the reactant, the transition state complex and the product using spread sheet (excel 2016). The dissociation barrier of cysteine side chain and guanine radical cation complex was calculated to be 0.0070 $E_{h.}$ Figure 16 shows the potential energy curve along the cysteinyl (S-H-O) guanyl coordinate.

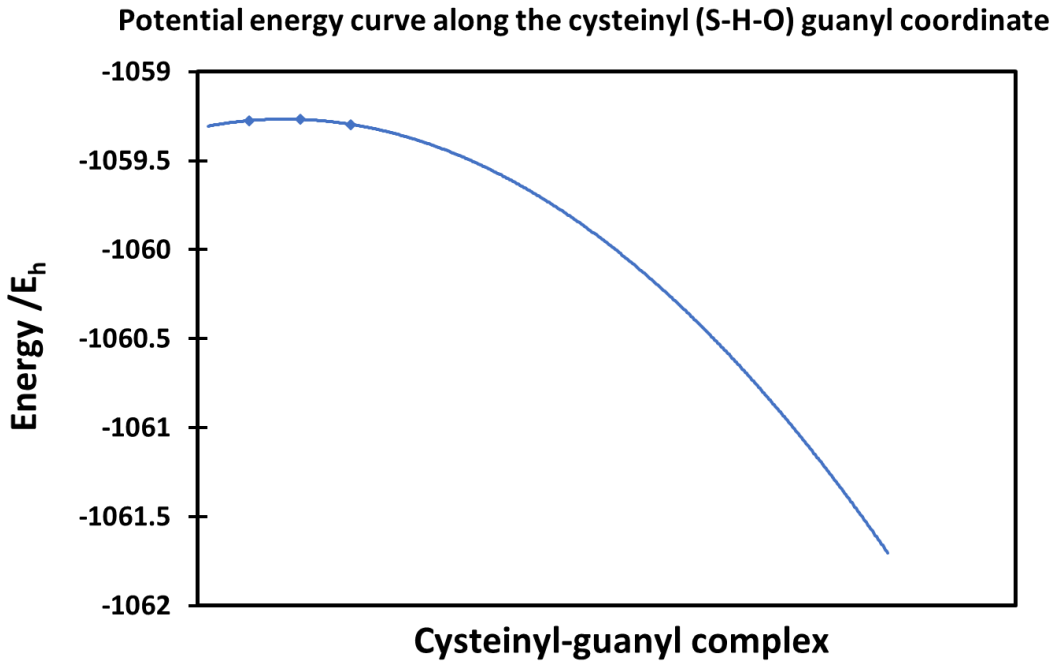

Figure 16: The potential energy curve along the cysteinyl (S-H-O) guanyl coordinate.

In the studies of tyrosine side chain and guanine radical cation complex, similar observations were made. In the reactant state all the spins were located on the guanine as shown in the Figure 17 below.

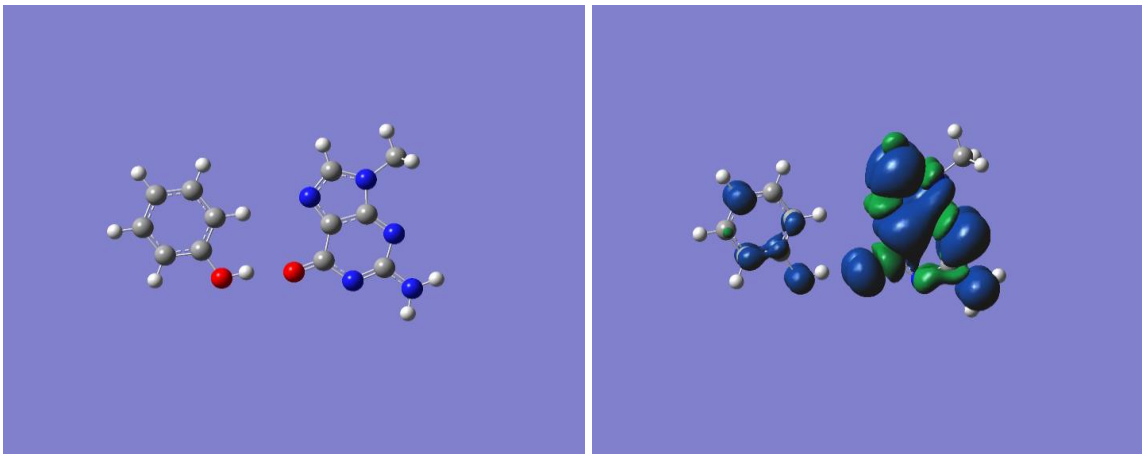

a **b**

Figure 17: Tyrosine side chain and guanine radical cation complex before electron transfer coupled with proton transfer with (a) showing atoms and (b) showing spin density

At the transition state complex, the spins were partly on both the amino acid side chain and the guanine moieties. Figure 18 show the transition state complex

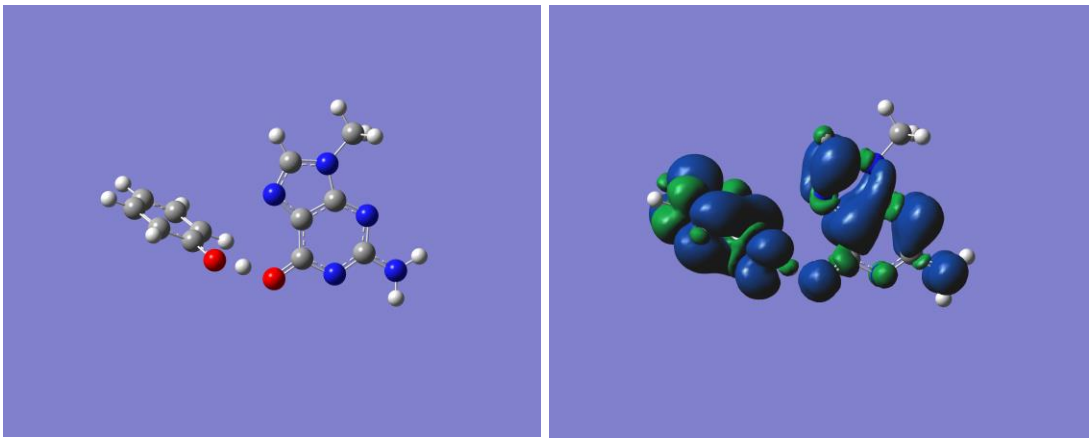

a **b**

Figure 18: Tyrosine side chain and guanine radical cation complex showing electron transfer coupled with proton transfer to guanine radical cation at the transition state

At the product state complex all the spins migrated to the amino acid side chain, indicating a complete transfer of hole from the guanine to the amino acid. Figure 19 shows both the molecular complex and the spin respectively.

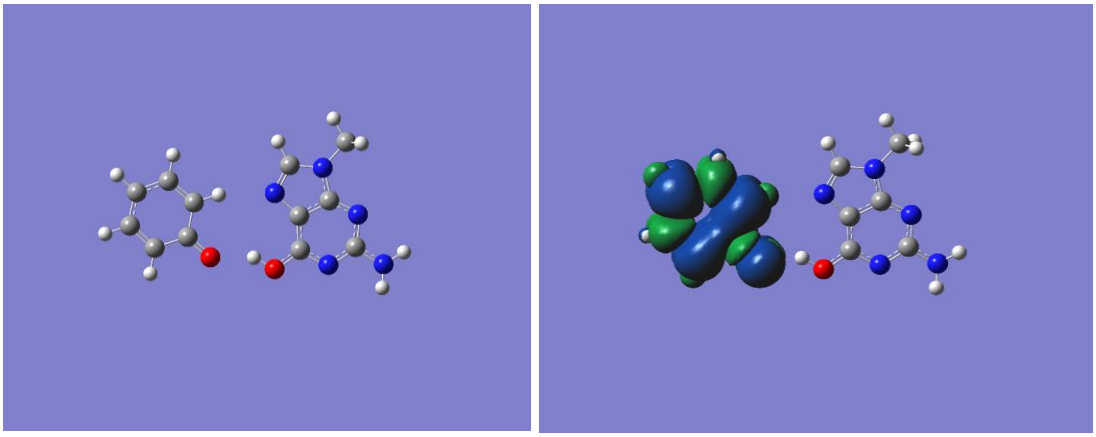

a **b**

Figure 19: Tyrosine side chain with guanine radical cation after electron transfer coupled with proton trasfer at the product state

The energies at various states were calculated from the Gaussian 09 program and tabulated below

Table 4: Calculated energies at the various states of the tyrosine side chain and guanine radical cation complexes.

Tyrosyl and guanyl complexes	Energies / E_h
Reactant	-888.7552
Transition State	-888.7487
Product	-888.7652

The potential energy curve along the tyrosine (O-H-O) guanyl coordinate was obtained by plotting the tyrosine side chain and guanine complexes of the reactant, the transition state complex and the product using a spreadsheet (Excel 2016). The dissociation barrier was calculated to be 0.0065 E_h. Figure 20 shows the potential curve along the tyrosinyl (O-H-O) guanyl coordinate.

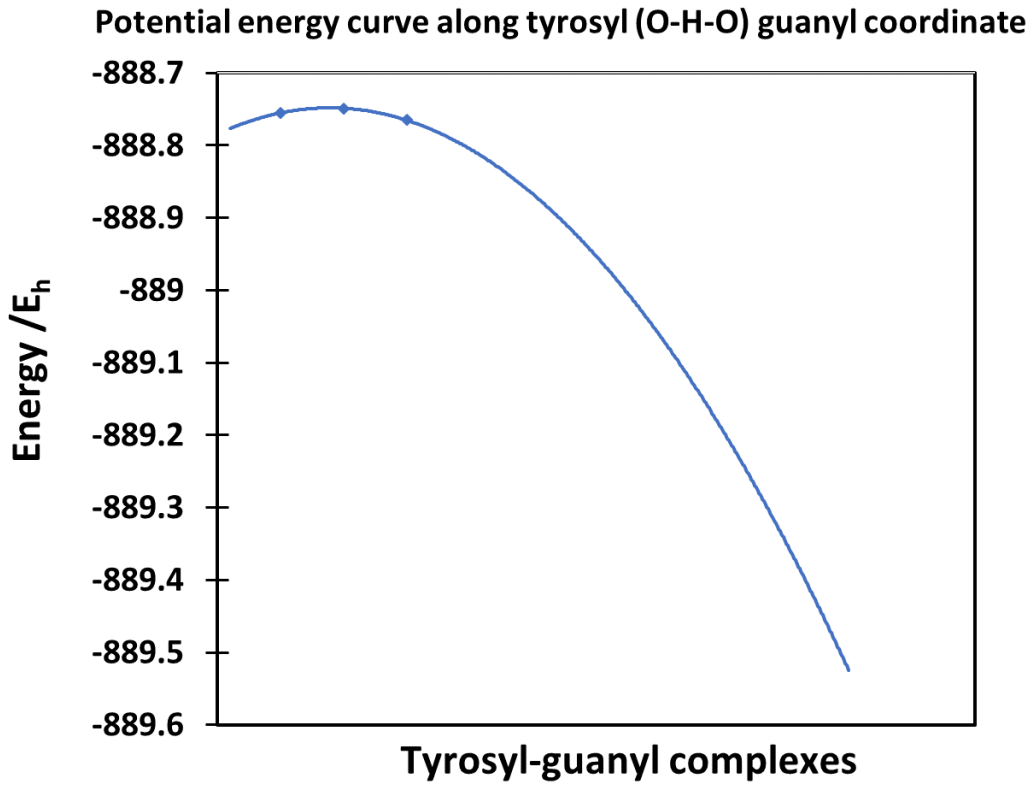

Figure 20: Potential energy curve along the tyrosinyl (O-H-O) guanyl coordinate

Similarly, histidine side chain and guanine radical cation complexes were investigated. In the reactant complex, before the transfers of electron and proton, all spin was shown to the guanine moiety as shown in Figures 21.

The geometry is represented by (a) and the spin densities by (b)

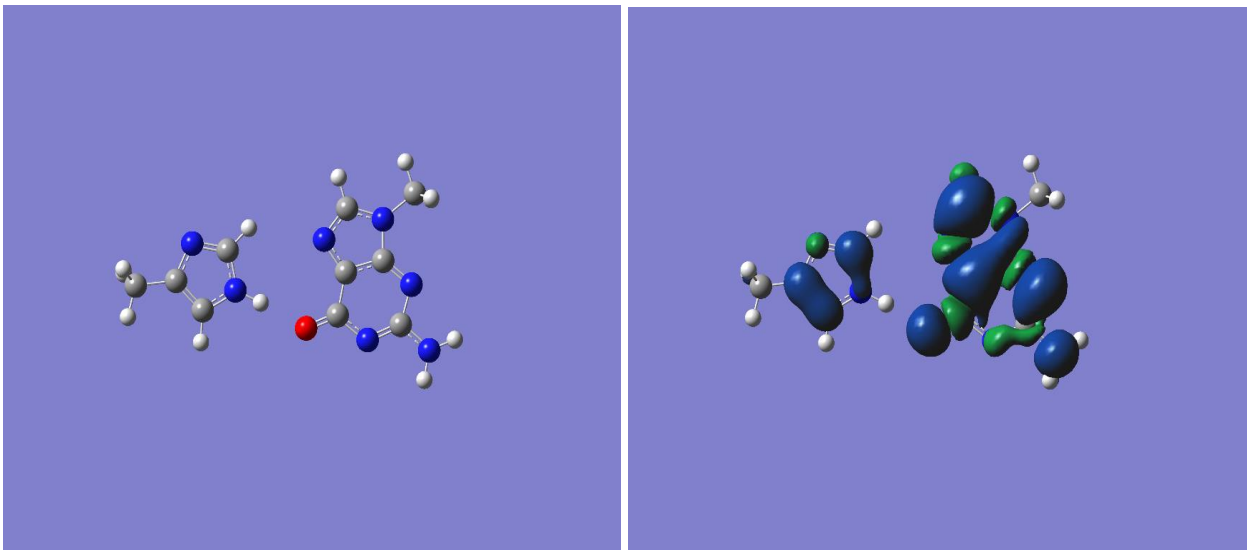

a **b**

Figure 21: Histidine side chain and guanine complex before electron transfer coupled with proton transfer with (a) showing atoms and (b) showing spin densities

At the transition state complex, significant amounts of the spin were located on the amino acid moiety as shown Figure 22 below

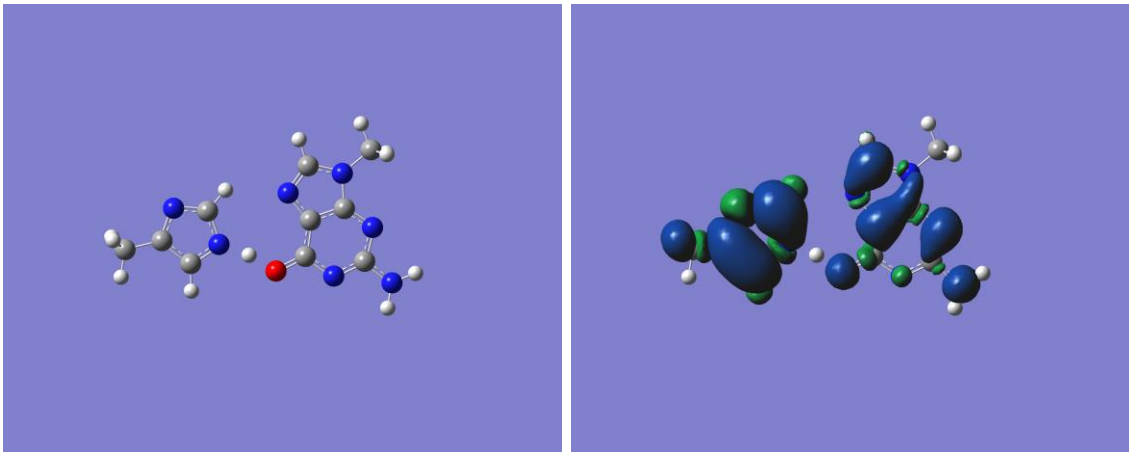

a **b**

Figure 22: Histidine side chain and guanine radical cation complex showing electron transfer coupled with proton transfer to guanine radical cation at the transition state

At the product state complex all the spin were located on the amino acid moiety as shown in Figures 23.

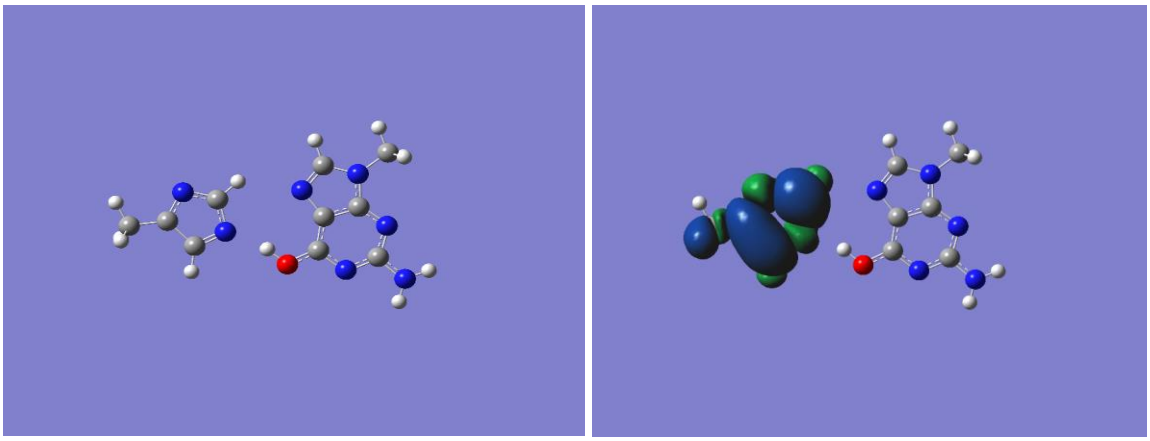

a **b**

Figure 23: Histidine side chain with guanine radical cation after electron transfer coupled with proton trasfer at the product state

The energies at various state were again calculated from the Gaussian 09 program and tableted below in Table 5.

Table 5: Calculated energies at the various state of the histidine side chain and guanine radical cation complexes

Histidinyl and guanyl complexes	Energies / E_h
Reactant	-846.8224
Transition State	-846.8111
Product	-846.8209

The potential energy curve along the histidinyl (N-H-O) guanyl coordinate was obtained by plotting the histidine side chain and guanine complexes of the reactant, the transition state

complex and the product using spread sheet (Excel 2016). The dissociation barrier was calculated to be 0.0113 E_h. Figure 24 shows the potential curve along the histidinyl (N-H-O) guanyl coordinate.

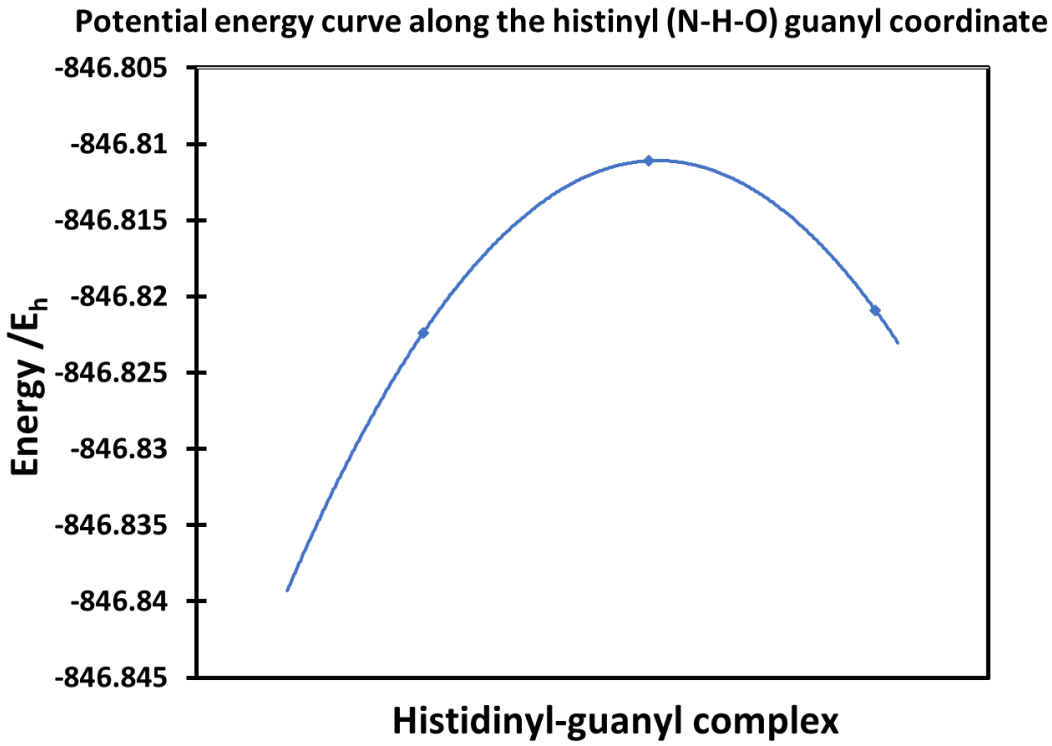

Figure 24: Potential energy curve along the histidinyl (N-H-O) guanyl coordinate

Lastly the interaction of amino acid side chain and guanine complex considered is for tryptophan. The reactant complex showed spins on both the amino acid side cain and the guanyl radical cation as shown in Figure 25 below

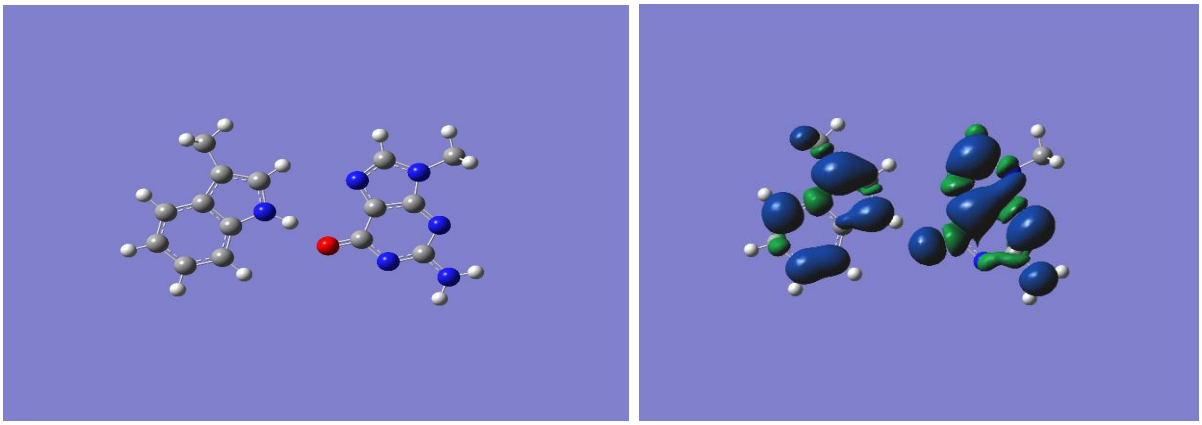

a **b**

Figure 25: Tryptophan side chain and guanine complex before electron transfer coupled with proton transfer with (a) showing atoms and (b) showing spin densities

The transition state showed similar characteristic even though much of the spin densities were located on the amino acid side chain as shown in Fgure 26 below

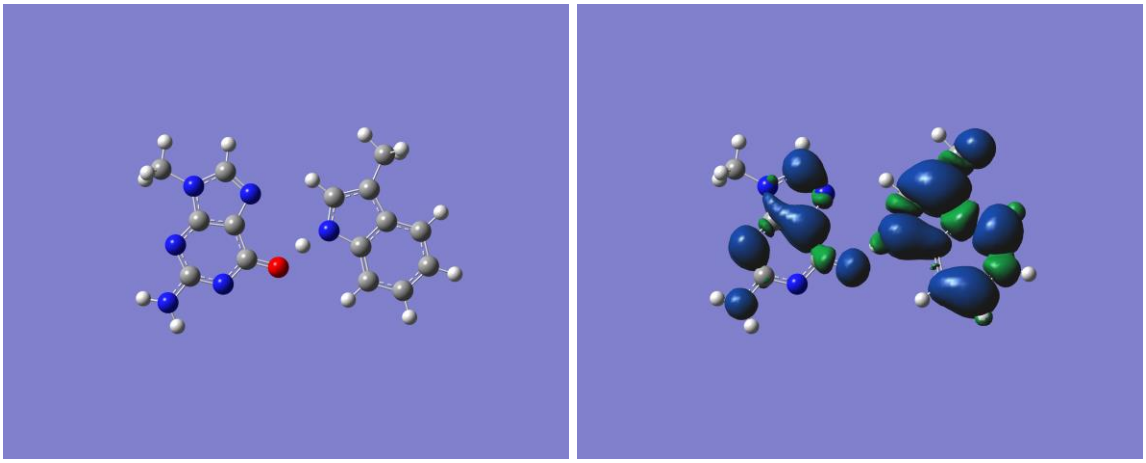

a **b**

Figure 26: Tryptophan side chain and guanine radical cation complex showing electron transfer coupled with proton transfer to guanine radical cation at the transition state

The product state showed all the spin trapped on the tryptophan side chain as shown in Figure 27 below

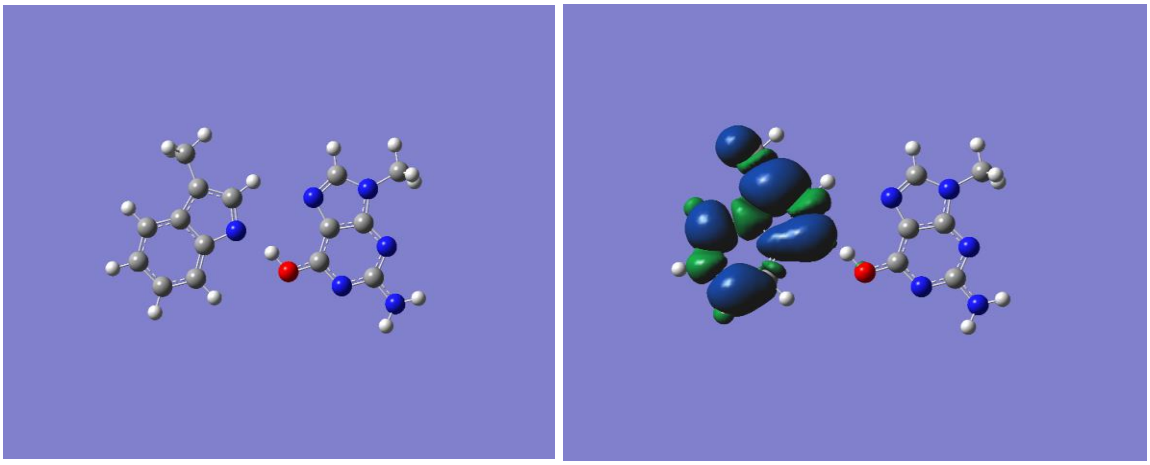

a **b**

Figure 27: Tryptophan side chain with guanine radical cation after electron transfer coupled with proton trasfer at the product state

The energies at various state were again calculated from the Gaussian 09 program and tableted below in Table 6.

Table 6: Calculated energies at the various state of the tryptophan side chain and guanine radical cation complexes

Tryptophanyl and guanyl complexes	Energies / E_h
Reactant	-984.4304
Transition State	-984.4267
Product	-984.4352

The potential energy curve along the tryptophanyl (N-H-O) guanyl coordinate was obtained by plotting the tryptophan side chain and guanine complexes of the reactant, the transition state complex and the product using spreadsheet (Excel 2016). The dissociation barrier was calculated to be 0.0037 E_h. Figure 28 shows the potential curve along the tryptophanyl (N-H-O) guanyl coordinate.

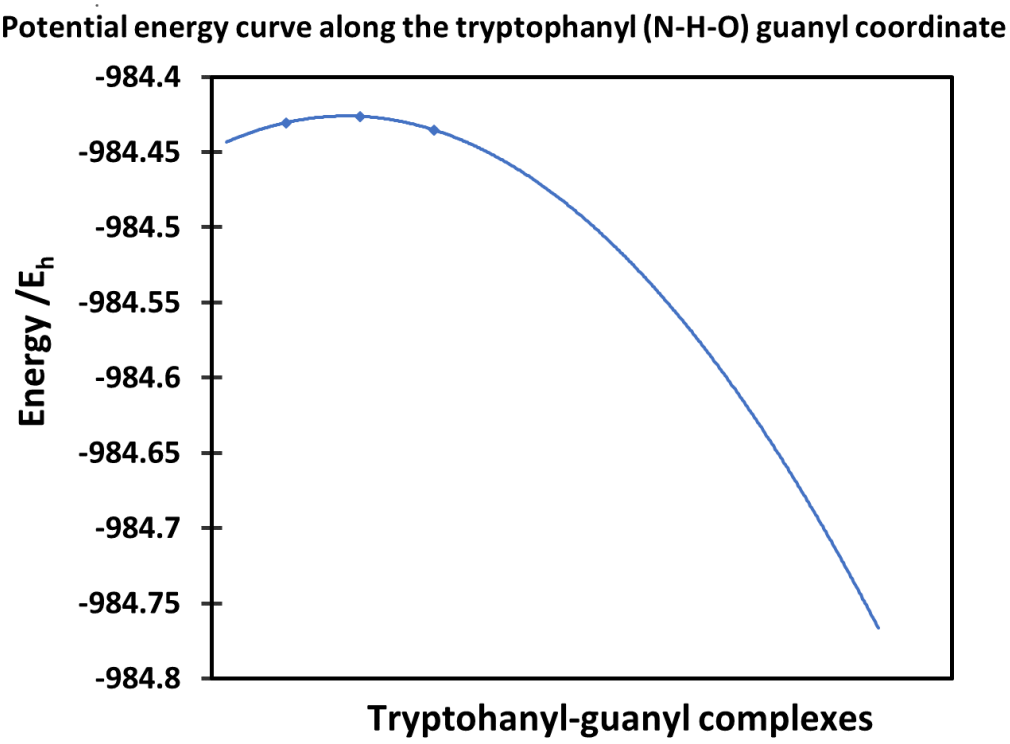

Figure 28: Potential energy curve along the tryptophanyl (N-H-O) guanyl coordinate

CHAPTER 4

CONCLUTION

Proton-coupled electron transfer (PCET) reactions between cysteine, tyrosine tryptophan, histidine side chain and guanine radical cation can occur. The energy barrier of these complexes is in the order 0.0113 E_h, > 0.0070 E_h, > 0.0065 E_h, > 0.0037 E_h for histidine,cysteine, tyrosine, and tryptophan side chain respectively.Therefore all four amino acids side chains studied here will reduce the guanine radical cation.

REFERENCES

1. Katerina, S.; V. Mudera.; and U. Cheema. Evolution of oxygen utilization in multicellular organisms and implications for cell signaling in tissue engineering. *J Tissue Eng*. **2011**, 2(1) 2041731411432365.
2. V. Lobo, A. Patil, A. Phatak and N. Chandra. Free radicals, antioxidants and functional foods: Impact on human health. *Pharmacogn Rev*. **2010**, 4(8), 118-128.
3. Valko, M.; Morris, H.; Cronin, M. T. Metal, Toxicity and Oxidative Stress. *Cur. Med. Chem* **2005**, *12*, 1161-1208.
4. Cadet, J.; Douki, T.; Pouget, J. P.; Ravanat, J. L.; Sauvaigo, S. Effect of UV and Visible Radiations on Cellular DNA *Curr. Probl. Dermatol* **2001,** 29, 62-73.
5. Cook, J. A.; Gius, D.; Wink, D. A.; Krishna, M. C.; Russo, A.; Mitchell, J. B. Oxidative Stress, Redox and Tumor Microenvironment. *Semin. Radiat. Onco*l, **2004**, 14,259-266.
6. Miura, Y. *J. Radiat. Oncol.* **2004**, *14*, 259-266.
7. Barry, H. *Bio Chem.J. Oxidative Stress and Cancer: Have we moved forward?* **2007**, *401*. 1-11.
8. Wiseman, H.; Halliwell, B. *Biochem. J.* Damage to DNA by Reactive Oxygen Species: Role in Inflammatory Disease and Progression of Cancer. **1996**, 313, 17-29.
9. Loft, S.; Larsen, P. N.; Rasmussen, A.; Fischer-Nielsen, A.; Bondesen, S.; Kirkegaard, P.; Rasmussen, L. S.; Ejlersen, E.; Tornoe, K.; Bergholdt, R. Oxidative DNA Damage after Transplanting of Liver and Small Intestines in Pigs. *Transplantation* **1995**, *59, 16-20.*
10. Lezza, A.; Mecocci, P.; Cormio, A.; Flint Beal, M.; Cherubini, A.; Cantatore, P.; Senin, U.; Gadaleta, M. N. *J. AntiAging Med* **1999**, *2*, 209-215.
11. Toyokuni, S. O.; Yodoi, J.; Hiai, H. Persistent Oxidative Stress in Cancer. *FEBS Lett*, **1995**, *358*, 1-3.
12. Cook, J. A.; Gius, D.; Wink, D. A.; Krishna, M. C.; Russo, A.; Mitchell, J. B. *Semin. Radiat. Oncol.*, **2004**, *14*, 259-266.
13. Jean-Luc Ravanat.; Thierry Douki.; Jean Cadet. Direct and indirect effects of UV radiation On DNA and its components. *Biology*. **2001**, 63, 88–102.
14. Shirley, R. O.; Work, L. Oxidative Stress and the use of Antioxidants in Stroke. *Antioxidants*,

2014, *3*, 472-501.

15. Xu, Y. J.; Kim, E. Y.; Demple, B. *J. Biol. Chem.*, **1998**, *273*, 28837-28844.
16. Steenken, S. Electron-Transfer-Induced Acidity/Basicity and Reactivity Changes of Purine and Pyrimidine Bases. Consequences of Redox Process for DNA Base Repair. *Free Rad Res Comm* **1992**, *16*, 349-379.
17. Genevieve, P.; Bernard. M. Guanine Oxidation: One- and Two-Electron Reactions. *Chempubsoc*. **2006,** 12(23), 6018-6030.
18. Anil, K.; Ventaka. P.; Michael. D. S. Hydroxyl Radical ($OH^{\bullet}$) Reaction with Guanine in an Aqueous Environment: A DFT Study. *J Phys Chem B*. **2011,** 115(50), 15129-15137.
19. Saito, I. N.; Nakatani, K.; Yoshioka, Y.; Yamaguchi, K.; Sugiyama, H. Mapping of the Hot Spots for DNA Damage by One-Electron Oxidation: Efficacy of GG Doublets and GGG Triplets as a Trap in Long-Range Hole Migration *J. Am Chem. Soc.*, **1998**, *120*, 12686 12687.
20. Douki, T. M.; Ravanat, J.-L.; Turesky, R. J.; Cadet, J. Measurement of 2,6-diamino-4-hydroxy-5-formamidopyrimidine and 8-oxo-7,8-dihydroguanine in isolated DNA exposed to gamma radiation in aqueous solution. *Carcinogenesis*, **1997**, *18*, 2385-2391.
21. Cadet, J.; Douki, T.; Gasparutto, D.; J-L. *Mutat*. Res. **2003,** 531.
22. Candeias, LP.; Steenken, S. Structure and acid-base properties of one-electron-oxidized deoxyguanosine, guanosine, and 1-methylguanosine *J Am Chem. Soc*. **1989;** 111: 1094-1099.
23. Close, D. M. Calculated pK_a's of the DNA Base Radical Ions. *J. Phys. Chem.*, **2013**, *117*, 473-480.
24. Roginskaya, M.; Bernhard, W.; Razskazovskiy, Y. Protection of DNA against Direct Radiation Damage by Complex Formation with Positively Charged Polypeptides. *Radiat. Res*.,**2006**, *166*, 9-18.
25. Drew, H. R.; Dickerson, R. E. Structure of a B-DNA Dodecamer. III. Geometry of Hydration. *J. Mol. Biol*. **1981**, 151 (3), 535-556.
26. Chen, S. H.; Liu, L.; Chu, X.; Zhang, Y.; Fratini, E.; Baglioni, P.; Faraone, A.; Mamontoy, E. Experimental Evidence of Fragile-to-Strong Dynamic Crossover in DNA Hydration Water. *J. Chem. Phys*. **2006**, 125, 171103.
27. Denisov, V. P.; Carlström, G.; Venu, K.; Halle, B. Kinetics of DNA Hydration. J. Mol. Biol.

1997, 268, 118-136.

28. Pal, S. K.; Zhao, L.; Zewail, A. H. Water at DNA Surfaces: Ultrafast Dynamics in Minor Groove Recognition. Proc. Natl. Acad. Sci. U. S. A. **2003**, 100 (14), 8113-8118.
29. Szyc, Ł.; Yang, M.; Nibbering, E. T. J.; Elsaesser, T. Ultrafast Vibrational Dynamics and Local Interactions of Hydrated DNA. Angew. Chem., Int. Ed. **2010**, 49 (21), 3598-3610.
30. Furse, K. E.; Corcelli, S. a. The Dynamics of Water at DNA Interfaces: Computational Studies of Hoechst 33258 Bound to DNA. J. Am. Chem. Soc. **2008,** 130 (39), 13103-13109.
31. Nolwenn, L. B.; John, J. W.; Andrew, J. Y. Jones.; Enrico, S.; Hannah, R. B.; Judy, H.; and Maxie, M. R. Using Hyperfine Electron Paramagnetic Resonance Spectroscopy to Define the Proton-Coupled Electron Transfer at Fe-S Cluster N2 in Respiratory Complex 1. *J. AM. Chem. Soc.* **2017**, 139, 16319-16326.
32. Liepinsh, E.; Otting, G.; Wüthrich, K. NMR Observation of Individual Molecules of Hydration Water Bound to DNA Duplexes: Direct Evidence for a Spine of Hydration Water Present in Aqueous Solution. *Nucleic Acids Res.* **1992**, 20 (24), 6549-6553.
33. Pal, S. K.; Zhao, L.; Zewail, A. H. Water at DNA Surfaces: Ultrafast Dynamics in Minor Groove Recognition. Proc. Natl. Acad. Sci. U. S. A. **2003,** 100 (14), 8113-8118.
34. Furse, K. E.; Corcelli, S. a. The Dynamics of Water at DNA Interfaces: Computational Studies of Hoechst 33258 Bound to DNA. J. Am. Chem. Soc. **2008,** 130 (39), 13103-13109.
35. Tao, N. J.; Lindsay, S. M.; Rupprecht, A. Structure of DNA hydration shells studied by Raman spectroscopy. *Biopolymers*, **1989**, *28*, 1019-1030.
36. La Vere, T.; Becker, D.; Sevilla, M. D. Yields of OH in gamma-irradiated DNA as a function of DNA hydration: hole transfer in competition with OH formation *Radiat. Res.*, **1996**, *145*, 673-80.
37. Gary, B. Schuster. Long-Range Charge Transfer in DNA I-II, *Topics in Current Chemistry*, **2004**.
38. Yuri, A. Berlin.; I, V. Kurnikov.; D, N. Bertran.; M, A. Ratner and A. L. Burin. DNA Electron Transfer Processes: Some Theoretical Notion. *Top. Curr. Chem.*, **2004,**237, 1–36.
39. Scott, R. Rajski and J. K. Barton. How Different DNA-Binding Proteins Affect Long-Range Oxidative Damage to DNA. *Biochemistry*, **2001**, 40 (18), 5556-5564.

40. Tobias, Cramer.; S, Krapf and T. Koslowski. Charge transfer through the nucleosome: a theoretical approach. *Phys. Chem. Chem. Phys.*, **2004**, 6, 3160-3166.
41. N, R. Jena.; P, C. Mishra and S. Suhai. Protection Against Radiation-Induced DNA Damage by Amino Acids: A DFT Study. *J. Phys. Chem. B*, **2009**, 113, 5633–5644.
42. Joseph, C. Genereux.; A, K. Boal and J. K. Barton. DNA-Mediated Charge Transport in Redox Sensing and Signaling. *J. Am. Chem. Soc.*, **2010**, 132, 891–905.
43. Paul, M. Cullis.; G, D. D. Jones.; M, C. R. Symons and J. S. Lea. Electron transfer from protein to DNA in irradiated chromatin *Nature*, **1987**, 330, 773–774.
44. Nunez, M. E.; K. T. Noyes and J. K. Barton. Oxidative charge transport through DNA in nucleosome core particles. *Chem. Biol.*, **2002**, 9 (4), 403-15.
45. Kazuhiko, Nakatani.; C, Dohno.; A, Ogawa and I. Saito. Suppression of DNA-Mediated Charge Transport by BamHI Binding. *Chem. Biol.*, **2002**, 9, 361–366.
46. Chad, C. Bjorklund and W. B. Davis. Attenuation of DNA charge transport by compaction into a nucleosome core particle. *Nucleic Acids Res.*, **2006,** 34, 1836-1846.
47. Davey, C A.; D, F. Sargent.; K, Luger.; A, W. Maeder and T, J. Richmond. Solvent mediated interactions in the structure of the nucleosome core particle at 1.9 a resolution. *J. Mol. Biol.*, **2002**, 319, 1097–1113.
48. Adams, G.E.; Aldraich, J. E.; Bisby, R. H.; Cundall, R. B.; Redpath, J. L.; and Willson, R. L. Selective Free Radical Reactions with Proteins and Enzymes: Reactions of Inorganic Radical Anions with Amino Acids. *Radiat. Res.* **1972**, 49, 278-289.
49. Jing Zhao.; H. Yang.; M. Zhang.; and Y. Bu. Interactions of Amino Acids with Oxidized Guanine in Gas Phase Associated with the Protection of Damaged DNA. *Chemphyschem*., **2013**, 14, 1031-1042.
50. K, N. Sutherland.; P, C. Mineau.; and G, Orlova. Radical-cationic gaseous amino acids: a theoretical study. *J. Phys. Chem*. A **2007**, 111 (32), 7906-14.
51. Levine, I. N., *Quantum Chemistry*. 7th ed.; Pearson: Boston, **2014.** 7-11.
52. Schrödinger, E. Quantisierung als Eigenwertproblem. *Annalen der Physik* **1926,** 79 (6), 489-527.
53. Levine, I. N., *Quantum Chemistry*. 7th ed.; Pearson: Boston, **2014**. 39-46.
54. Witt, C. Hamiltonian Operator. Compendium of Quantum Physics. Springer Berlin. **2009**.

55. Levine, I. N., *Quantum Chemistry*. 7th ed.; Pearson: Boston, **2014**. 232-237.
56. Teschl, G. Mathematical Methods in Quantum Mechanics; With Applications to Schrödinger Operators, American Mathematical Society, **2009**.
57. Courant, R.; Hilbert, D. Methods of Mathematical Physics, **1962**, Volume I, Wiley Interscience
58. Hartree, D. R. The wave mechanics of an atom with a non-Coulomb central field. Part I: theory and methods. *Proc. Cambridge. Philos. Soc*. **1928**, 24 (1), 89-110.
59. Hartree, D. R. The Wave Mechanics of an Atom with a Non-Coulomb Central Field II: Some Results and Discussion. *Proc. Cambridge Phil. Soc.* **1927**, 24, 111.
60. Slater, J. C.; Atomic Shielding Constants. *Phys. Rev.* **1930,** 36 (1), 57-64.
61. Roothaan, C. C. J. Self-Consistent Field Theory for Open Shells of Electronic Systems. *Rev. Mod. Phys.* **1960,** *32* (2), 179-185.
62. Fock, V. A. Näherungsmethode zur Losung des quanten-mechanischen Mehrkorperprobleme Z. Phys. 1930, 61 (1), 126-148.
63. Ramachandran, K. I.; G. Deepa.; K. Namboori. Computational Chemistry and Molecular Modeling. Springer **2008**.
64. Roothaan, C. C. New Developments in Molecular Orbital Theory, Reviews of Modern Physic. **1951**, 23, 69-89.
65. Hall, G. G. The Molecular Orbital Theory of Chemical Valency. VIII. A Method of Calculating Ionization Potentials. **1951**, 205, 541-552.
66. Kohn, W.; Becke, A. D.; Parr, R. G. Density Functional Theory of Electronic Structure. *J. Phys. Chem.* **1996**, 100, 12974.
67. Hohenberg, P.; Kohn, W. Inhomogeneous electron gas. *Phys. Rev*. **1964**, 136, B864.
68. Kohn, W.; Sham, L. J. Self-Consistent Equations including Exchange and Correlation Effects. *Phys. Rev*. **1965**, 140, A1133.
69. Becke, A. D., Density-functional exchange-energy approximation with correct asymptotic behavior. *Phys. Rev. A* **1988,** 38 (6), 3098-3100.
70. Becke, A. D. Density-functional thermochemistry. III. The role of exact exchange. *J. Chem. Phys.* **1993,** 98, 5648.

71. Halkier, A.; Helgaker, T.; Jørgensen, P.; Klopper, W.; Olsen, J. Basis-set convergence of the energy in molecular Hartree-Fock calculations. *Chem. Phys. Lett*, **1999**, 302 437-447.
72. Boys, S. F.; Bernardi, F. Electronic Wavefunction. *Mol Phy*, **1950**. 19. 559.
73. Peterson, K. A.; Woon, D. E.; Dunning, T. H., Jr., Benchmark calcutations with correlated molecular wave functions. IV. The classical barrier height of the H+H2 --> H2+H reaction. *J. Chem. Phys.* **1994,** 100 (10), 7410-7415.
74. Helgaker, T.; Klopper, W.; Koch, H.; Noga, J., Basis-set convergence of correlated calculations on water. *J. Chem. Phys.* **1997,** 106 (23), 9639-9646.
75. Halkier, A.; Helgaker, T.; Jørgensen, P.; Klopper, W.; Koch, H.; Olsen, J.; Wilson, A. K., Basis-set convergence in correlated calculations on Ne, N_2, and H_2O. *Chem. Phys. Lett.* **1998,** 286 (3), 243-252.
76. Dunning, T. H. Jr. Gaussian basis sets for use in correlated molecular calculations. I. The atoms boron through neon and hydrogen. *J. Chem. Phys*. **1989**, 90(2), 1007-1023.
77. Kendall, R. A.; Dunning, T. H., Jr.; Harrison, R. J. Electron affinities of the first-row atoms revisited. Systematic basis sets and wave functions. *J. Chem. Phys*. **1992**, 96(9), 6796-6806.
78. Hartree, D. R. The Wave Mechanics of an Atom with a Non-Coulomb Central Field II: Some Results and Discussion. *Proc. Cambridge Phil. Soc.* **1927**, 24, 111.
79. Gaussian 09 Revision E.01, Gaussian, Inc., Wallingford CT, **2009.**
80. Jamie, R. Milligan.; J. A. Aguilera.; O. Hoang.; A. Ly.; N. Q. Tran.; and John F W. Peptides repair of oxidative DNA damage. *Chem. Soc***. 2004** 126, 1682.

VITA

EDWARD ACHEAMPONG

Education:	M.S. Chemistry, East Tennessee State University (ETSU), Johnson City, Tennessee, USA. (2016-2018)
	BSc. Chemistry, (Second Class Honors, Upper Division), University of Cape Coast, Ghana, West Africa. (2011-2015)
Experience:	Graduate Teaching Assistant, Chemistry Department, East Tennessee State University, Johnson City, Tennessee, USA. (2016-2018)
	Teaching Assistant, Chemistry Department, School of Physical Sciences, University of Cape Coast. Ghana, West Africa. (2015-2016)